

Sensor Calibration for Off-the-Grid Spectral Estimation

Yonina C. Eldar*

Wenjing Liao †

Sui Tang ‡

July 12, 2017

Abstract

This paper studies sensor calibration in spectral estimation where the true frequencies are located on a continuous domain. We consider a uniform array of sensors that collects measurements whose spectrum is composed of a finite number of frequencies, where each sensor has an unknown calibration parameter. Our goal is to recover the spectrum and the calibration parameters simultaneously from multiple snapshots of the measurements. In the noiseless case, we prove uniqueness of this problem up to certain trivial, inevitable ambiguities with an infinite number of snapshots as long as there are more sensors than frequencies based on an algebraic method. We then analyze the sensitivity of this approach with respect to the number of snapshots and noise. We next propose an optimization approach that makes full use of the measurements and consider a non-convex objective over all calibration parameters and Toeplitz matrices. This objective is non-negative and continuously differentiable. We prove that, in the case of infinite snapshots of noiseless measurements, the objective vanishes only at the equivalent solutions to the true calibration parameters and the measurement covariance matrix with all calibration parameters being 1 which exhibits a Toeplitz structure. The objective is minimized using Wirtinger gradient descent which we prove converges to a critical point. We show empirically that this critical point provides a good approximation of the true calibration parameters and the underlying frequencies.

1 Introduction

High-performance systems in signal processing often require precise calibration of sensors, however, such advanced sensors can be very expensive and difficult to build. It is, therefore, beneficial to use measurements themselves to adjust calibration parameters and perform signal recovery simultaneously.

We consider sensor calibration in spectral estimation where the frequencies of interest are located on a continuous domain. In particular, suppose a uniform array of N sensors collects measurements whose spectrum is composed of s spikes located at $\mathcal{S} := \{\omega_j \in [0, 1]\}_{j=1}^s$ with amplitudes $x(t) := \{x_j(t)\}_{j=1}^s \in \mathbb{C}^s$ at time t . Each sensor has an unknown calibration parameter g_n , $n = 0, \dots, N - 1$. The measurement vector at the array output can then be written as

$$y_e(t) = GAx(t) + e(t), \quad (1)$$

where $y_e(t) \in \mathbb{C}^N$ and $y_{e,n}(t)$ is the noisy measurement collected by the n -th sensor at time t , $G = \text{diag}(g) \in \mathbb{C}^{N \times N}$ with $g = \{g_n\}_{n=0}^{N-1} \in \mathbb{C}^N$, $e(t) \in \mathbb{C}^N$ is the noise vector at time t , and

*Department of EE Technion, Israel Institute of Technology, Haifa. Email: yonina@ee.technion.ac.il

†School of Mathematics, Georgia Institute of Technology. Email: wenjing.liao@math.gatech.edu

‡Department of Mathematics, Johns Hopkins University. Email: stang@math.jhu.edu

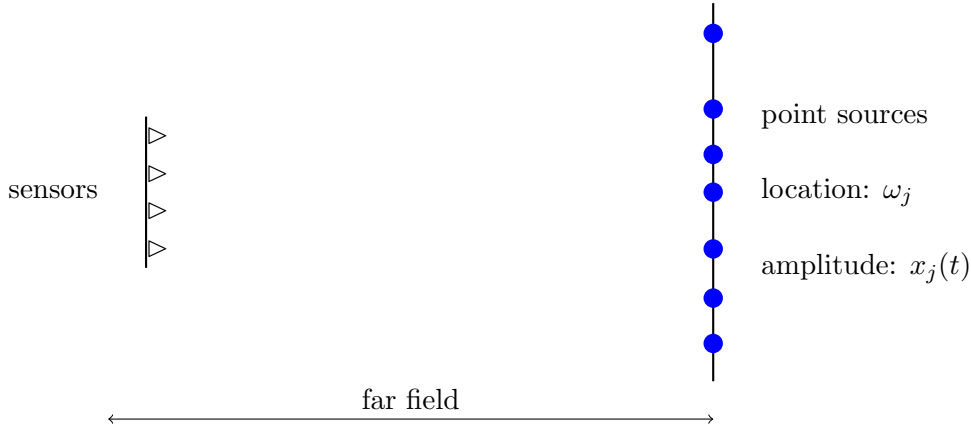


Figure 1: Source localization in array imaging

$A \in \mathbb{C}^{N \times s}$ is the sensing matrix defined by

$$A_{n,j} = \frac{1}{\sqrt{N}} e^{2\pi i n \omega_j}. \quad (2)$$

Our goal is to recover the spectrum \mathcal{S} and the calibration parameters g simultaneously from noisy measurements $\{y_e(t), t \in \Gamma\}$ where $L := \#\Gamma$ is the number of snapshots.

Spectral estimation modeled by (1) is a fundamental problem in imaging and signal processing. It is widely used in speech analysis, direction of arrival (DOA) estimation, array imaging, and remote sensing. For example, in array imaging (see Fig. 1), we assume there are s sources located at $\{\omega_j\}_{j=1}^s$ with amplitudes $\{x_j(t)\}_{j=1}^s$, and set a uniform array of sensors to collect measurements $\{y_e(t), t \in \Gamma\}$. Our goal is to recover the source locations and the sensor calibration parameters simultaneously from the measurements.

When all sensors are perfectly calibrated, many methods have been proposed to recover frequencies located on a continuous domain, such as Prony's method [20], MUSIC [22, 23], ESPRIT [21], ℓ_1 minimization [3, 27], and the greedy algorithms [8, 10]. We refer the reader to [9, 24] for a comprehensive review. In this paper, the problem is complicated by the fact that each sensor has an unknown calibration parameter.

The calibration problem modeled by (1) has been considered in [19, 31, 32, 11]. Assume that, the underlying frequencies have random and uncorrelated amplitudes, frequencies and noises are independent, and noises at different sensors are uncorrelated. In [19], Paulraj and Kailath investigated DOA estimation using a uniform linear array in the presence of unknown calibration parameters. By exploiting the Toeplitz structure of the measurement covariance in the case of perfect sensors (which we refer to the case that all calibration parameters are 1), they proposed an algebraic method relying on least square solutions of two linear systems of equations for the calibration amplitudes and phases, respectively. However, phase wrapping in the set of equations for the calibration phase estimation is not taken into account and can degrade the DOA estimator performance (see Section 3.1). This method is called the full algebraic method in our paper. A similar approach is followed in [32]. In [13], Li and Er analyzed the full algebraic method with finite snapshots of measurements. They show that the average bias is nonzero, and that if the problem of phase wrapping is resolved, then the variance for the calibration phases is $O(1/\sqrt{L})$ where L is the number of snapshots. However, it remains unclear how to resolve phase wrapping in the full algebraic method. In addition, their results in [13] do not cover sensitivity to noise, and sensitivity in the spectral estimation. In [31], Wylie, Roy, and Schmitt proposed a partial algebraic method which successfully avoids the problem of phase

wrapping by removing redundancy in the linear system. A shortcoming of their approach is that a large part of the measurements are not taken into account in the recovery process.

In [11], an alternating algorithm is proposed by Friedlander and Weiss for the same calibration problem modeled by (1). This algorithm is based on a two-step procedure. First, one assumes that the calibration parameters are known, and estimates the frequencies through the MUSIC algorithm. Then one solves an optimization problem to obtain the best calibration parameters based on the recovered frequencies. The essential idea of this algorithm is alternating minimization, but no performance guarantee is provided. In addition, it does not perform as well as the partial algebraic method in numerical experiments.

Recently, many works address the following single-snapshot calibration problem:

$$y = \text{diag}(g)Ax_0 + e \quad (3)$$

where $g \in \mathbb{C}^N, x_0 \in \mathbb{C}^M$ are unknown calibration parameters and signal of interest, $A \in \mathbb{C}^{N \times M}$ is a given sensing matrix, $e \in \mathbb{C}^N$ represents noise, and $y \in \mathbb{C}^N$ is the measurement vector [1, 17, 16]. The goal is to recover g and x_0 from y . This problem is solved using a lifting technique in [1, 17], and non-convex optimization in [16], respectively. Performance guarantees are established in the case where g lies in a known subspace, and A is random Gaussian [1, 17] or random partial DFT matrix [17]. In spectral estimation, sensing matrices are not random Gaussian. The random partial DFT matrices are more closely related, but one has to discretize the frequency domain with grid spacing equal to $1/N$ in order to generate such sensing matrices. Here we do not discretize the frequency domain in order to avoid gridding errors [8, 10]. In [5], Chi considers a slightly different single-snapshot model:

$$y = \text{diag}(g)Ax \quad (4)$$

where $g \in \mathbb{C}^N$ contains unknown calibration parameters, A is the same as (2), $x \in \mathbb{C}^s$ is an unknown amplitude vector, and $y \in \mathbb{C}^N$ is the measurement vector. The goal is to recover g , x , and the frequencies $\{\omega_j\}_{j=1}^s$ from y . This problem is the same as our model (1) with single snapshot. Chi solves it using a lifting technique and atomic norm minimization, and proves that, in the noiseless case where g lies in a random subspace of dimension K with a coherence parameter μ , and if the underlying frequencies are separated by $4/N$, then exact recovery is guaranteed with a high probability as long as $N \geq C\mu K^2 s^2$ up to a log factor.

After sensors are built, it is usually cheap to take multiple snapshots of measurements. This paper studies the calibration problem modeled by (1) with multiple snapshots. In comparison with the works in [1, 5, 17, 16], we remove the assumption that g lies in a known subspace. Instead we utilize the Fourier structure and take advantage of the multiple snapshots. In addition, we only require more sensors than frequencies, namely, $N > s$.

1.1 Our contributions

We begin by studying uniqueness of the calibration problem modeled by (1) and propose several algorithms for signal recovery. We show there are certain inevitable ambiguities in (1). We characterize all trivial ambiguities, and prove that, both the spectrum and the calibration parameters are uniquely determined from infinite snapshots of noiseless measurements up to a trivial ambiguity, as long as there are more sensors than frequencies. Our proof is based on the algebraic methods proposed in [19, 31]. We then present a sensitivity analysis of the partial algebraic method [31] with respect to the number of snapshots L and noise level σ . In particular, Theorem 2 shows that, if the underlying frequencies are separated by $1/N$, then the reconstruction error of calibration parameters in the partial algebraic method is $O\left(\frac{C_1 + C_2 \max(\sigma, \sigma^2)}{\sqrt{L}}\right)$ for

some $C_1, C_2 > 0$. This rate is verified by numerical experiments. As for frequency localization, we prove that, the noise-space correlation function whose s smallest local minima correspond to the recovered frequencies in the MUSIC algorithm, is perturbed at most by $O\left(\frac{C_3 + C_4 \max(\sigma, \sigma^2)}{\sqrt{L}}\right)$ for some $C_3, C_4 > 0$.

The partial algebraic method in [31] only exploits partial entries of the measurement covariance matrix and the full algebraic method in [19] is affected by phase wrapping. We therefore propose an optimization approach to make full use of the measurements. We consider an objective function composed of two terms: one is a quadratic loss and the other is a penalty which prevents calibration parameters going to ∞ and frequency amplitudes decreasing to 0 (or vice versa). This objective is continuously differentiable but non-convex. We propose minimizing it over all possible calibration parameters and Toeplitz matrices. The optimization problem is solved by Wirtinger gradient descent [4]. We prove that, Wirtinger gradient descent converges to a critical point, and show empirically that this critical point provides a good approximation to the true calibration parameters and the underlying frequencies.

Finally we perform a systematic numerical study to compare the partial algebraic method [31], the alternating method [11], and our optimization approach. With respect to the stability to L and σ , our algorithm appears to have the best performance.

In summary, the main contributions of this paper are (i) characterizing all trivial ambiguities of the calibration problem modeled by (1) and proving uniqueness up to trivial ambiguities; (ii) presenting a sensitivity analysis of the partial algebraic method; (iii) proposing an optimization approach with superior numerical performance.

1.2 Related work

Recently, many interesting works have addressed the single-snapshot calibration problem modeled by (3) where the goal is to recover g and x simultaneously from y . Without additional assumptions, solutions to this problem are not unique since there are more unknowns than equations. In [1], Ahmed, Recht, and Romberg assume that g lies in a known subspace, and use a lifting technique to transform the problem into that of recovering a rank-one matrix from an underdetermined system of linear equations. They prove explicit conditions under which nuclear minimization is guaranteed to recover the original solution in the case where A is a random Gaussian matrix. In [17], Ling and Strohmer extend the framework in [1] to allow sparse signals with a random Gaussian matrix or random partial DFT matrix. The latter case is closely related to spectral estimation, but one has to discretize the frequency domain with grid spacing equal to $1/N$ in order to generate a partial DFT matrix. It is well known that, when the underlying frequencies are on a continuous domain, this discretization may cause gridding errors [6, 8, 10].

Since the lifting technique greatly increases the computational complexity, many non-convex optimization approaches are proposed to address problems in signal processing, such as phase retrieval [4, 2, 29, 25], dictionary recovery [26], blind deconvolution [16], and low-rank matrix estimation [33]. In [16], Li et al. formulate a non-convex optimization problem for the calibration problem modeled by (3), and solve it with a two-step scheme composed of a good initialization and gradient descent [16]. Performance guarantees are proved when g lies in a known subspace and A is a random Gaussian matrix. This theory does not apply to spectral estimation since the sensing matrix is not random Gaussian.

In array imaging, it is natural to consider multiple snapshots. The work in [14] addresses the following model:

$$Y = \text{diag}(g)AX_0 \tag{5}$$

where $g \in \mathbb{C}^N$, $X_0 \in \mathbb{C}^{M \times L}$ are unknown calibration parameters and signals in L snapshots, $A \in \mathbb{C}^{N \times M}$ is a given sensing matrix, $E \in \mathbb{C}^{N \times L}$ represents noise, and $Y \in \mathbb{C}^{N \times L}$ is the measurement matrix in L snapshots. In [14], Li, Lee and Bresler prove uniqueness up to a scaling ambiguity for generic signals X_0 and a generic sensing matrix A provided that $N > M$ and $\frac{N-1}{N-M} \leq L \leq M$. In the case where X_0 has s non-zero rows, uniqueness is proved for generic signals with s non-zero rows and a generic sensing matrix A provided that $N > 2s$ and $\frac{N-1}{N-2s} \leq L \leq s$. These conditions are optimal in terms of sample complexity. However, the theory in [14] does not apply to our case for the following reasons: (i) our sensing matrix defined in (2) is unknown, since it depends on the unknown frequencies; (ii) even if we discretize the frequency domain and approximate every frequency by the nearest grid point to fit the model (5), the sensing matrix is not generic. In comparison, our uniqueness results consider the structure of Fourier measurements but involve infinite snapshots of measurements. It is interesting to study the optimal sample complexity in our case, which we leave for future work.

1.3 Organization and Notation

This paper is organized as follows. Uniqueness results are described in Section 2.1. The partial algebraic method and its sensitivity analysis are presented in Section 3. Section 4 considers our optimization approach and its convergence to a critical point. Numerical simulations are presented in Section 5. We conclude and discuss future research directions in Section 6. Most proofs are relegated to the Appendices.

Throughout the paper we use s, N, L to denote the number of frequencies, the number of sensors, and the number of snapshots respectively. The expression $C = (A \ B)$ horizontally concatenates matrices A and B , while $C = (A; B)$ vertically concatenates them. For $x \in \mathbb{C}^N$, $\sum x := \sum_{j=1}^N x_j$, and $\text{diag}(x)$ is the $N \times N$ diagonal matrix whose diagonal is x . We use $|x| \in \mathbb{R}^N$ and $\angle x \in \mathbb{R}^N$ to denote the magnitude and phase vectors of x respectively such that $|x|_j = |x_j|$ and $(\angle x)_j = \angle x_j, j = 1, \dots, N$. For convention, we let $(\angle x)_j \in [-\pi, \pi)$. For an arbitrary angle θ , we assume $(\theta \bmod 2\pi) \in [-\pi, \pi)$. The dynamic range of x is the ratio between the largest amplitude and the smallest amplitude of x , denoted by $\text{DR}_x := \max_i |x_i| / \min_i |x_i|$. For $X \in \mathbb{C}^{N \times N}$, we use $\text{diag}(X)$ to denote the main diagonal of X , $\text{diag}(X, k), k > 0$ to denote the k th diagonal of X above the main diagonal, and $\text{diag}(X, k), k < 0$ to denote the k th diagonal of X below the main diagonal. The notation $\|X\|$ and $\|X\|_F$ represent the spectral norm and the Frobenius norm of X , respectively. The expression $A \preceq B$ for two square matrices A and B of the same size means $B - A$ is positive semidefinite. The expression $a \lesssim b$ for two scalars a and b means $a \leq Cb$ with a constant C independent of a, b . We use $\mathbf{0}$ to denote the null vector or the null matrix.

2 Uniqueness

2.1 Trivial ambiguity and uniqueness

In the case of a single snapshot, uniqueness does not exist since there are fewer measurements (N) than unknowns ($N + 2s$). After sensors are built, it is usually cheap to take multiple snapshots. For uniqueness we study the case with infinite snapshots of noiseless measurements. Clearly certain trivial ambiguities between the spectrum and the calibration parameters are inevitable. For example, one can add a gain to $x(t)$ and then divide it out in g , so that there is always a gain ambiguity. Similarly, there is always a shift ambiguity in the frequencies since we can shift all frequencies by a constant and all this will do is adding a phase modulation to g . In the next definition, we define the trivial ambiguities in the problem:

Definition 1 (Trivial ambiguity). *Let $\{g, \mathcal{S}, x(t)\}$ be a solution to the calibration problem modeled by (1). Then $\{\tilde{g}, \tilde{\mathcal{S}}, \tilde{x}(t)\}$ is called equivalent to $\{g, \mathcal{S}, x(t)\}$ up to a trivial ambiguity if there exist $c_0 > 0, c_1, c_2 \in \mathbb{R}$ such that*

$$\begin{aligned}\tilde{g} &= \{\tilde{g}_n = c_0 e^{i(c_1 + nc_2)} g_n\}_{n=0}^{N-1} \\ \tilde{\mathcal{S}} &= \{\tilde{\omega}_j : \tilde{\omega}_j = \omega_j - c_2/(2\pi)\}_{j=1}^s \\ \tilde{x}(t) &= x(t)c_0^{-1}e^{-ic_1t}.\end{aligned}$$

To proceed we make the following assumptions on the statistics of the frequencies (or sources in array imaging) and noises:

A1 Calibration parameters satisfy $|g_n| \neq 0, n = 0, \dots, N - 1$.

A2 Sources and noises have zero mean: $\mathbb{E}x(t) = \mathbf{0}$ and $\mathbb{E}e(t) = \mathbf{0}$.

A3 Sources are uncorrelated such that $R^x := \mathbb{E}x(t)x^*(t) = \text{diag}(\{\gamma_j^2\}_{j=1}^s)$.

A4 Sources and noises are independent, i.e., $\mathbb{E}x(t)e^*(t) = \mathbf{0}$.

A5 Noises at different sensors are uncorrelated so that $\mathbb{E}e(t)e^*(t) = \sigma^2 I_N$ where σ represents noise level.

Define

$$f_n = \frac{1}{N} \sum_{j=1}^s \gamma_j^2 e^{2\pi i n \omega_j}, \quad n = 0, \dots, N - 1 \quad (6)$$

which is sufficient to recover all frequencies by standard spectral estimation. Notice that $f_0 = \sum_{j=1}^s \gamma_j^2 > 0$. In the case of infinite snapshots, uniqueness of the calibration problem exists up to a trivial ambiguity as long as $|f_1| > 0$. This condition is sufficient to guarantee that the sub-diagonal entries in the covariance measurement do not vanish. If the frequency amplitudes $\{\gamma_j^2\}_{j=1}^s$ are generic, then we have $|f_1| > 0$ almost surely.

Theorem 1. *Suppose $|f_1| > 0$ and $N \geq s + 1$. Let $\{g, \mathcal{S}, x(t)\}$ be a solution to the calibration problem modeled by (1). If there is another solution $\{\tilde{g}, \tilde{\mathcal{S}}, \tilde{x}(t)\}$, then $\{\tilde{g}, \tilde{\mathcal{S}}, \tilde{x}(t)\}$ is equivalent to $\{g, \mathcal{S}, x(t)\}$ up to a trivial ambiguity.*

Theorem 1 guarantees uniqueness when $f_1 \neq 0$. In general, for $k = 1, \dots, N - 1$, we have $R_{l+k,l}^y = \alpha_{l+k}\alpha_l e^{i(\beta_{l+k} - \beta_l)} f_k$ where $l = 0, \dots, N - k - 1$. As long as $|f_k| \neq 0$, we can compute $R_{l+k+1,l+1}^y / R_{l+k,l}^y$ for $l = 0, \dots, N - k - 2$, which results in the following system of linear equations

$$\beta_{l+k+1} - \beta_{l+k} - \beta_{l+1} + \beta_l \equiv \angle R_{l+k+1,l+1}^y / R_{l+k,l}^y \pmod{2\pi} \quad (7)$$

for $l = 0, \dots, N - k - 2$. Here $a \equiv b \pmod{c}$ means a is equal to b modulo c . We can then write these $N - k - 1$ linear equations (7) in matrix form

$$\Phi_k \beta \equiv \delta_k \pmod{2\pi},$$

where

$$\Phi_1 = \begin{bmatrix} 1 & -2 & 1 & 0 & \dots & 0 & 0 & 0 \\ 0 & 1 & -2 & 1 & \dots & 0 & 0 & 0 \\ & & & \dots & & & & \\ & & & \dots & & & & \\ & & & \dots & & & & \\ 0 & 0 & 0 & 0 & \dots & 1 & -2 & 1 \end{bmatrix} \in \mathbb{C}^{(N-2) \times N},$$

Indeed, the (m, n) entry is

$$R_{m,n}^y = \frac{g_m \bar{g}_n}{N} \sum_{j=1}^s \gamma_j^2 e^{2\pi i \omega_j (m-n)} = g_m \bar{g}_n f_{m-n}. \quad (12)$$

The following lemma shows that g and f are uniquely determined from R^y up to a trivial ambiguity as long as f_1 does not vanish:

Lemma 1. *Suppose $|f_1| > 0$. If there is another set $\{\tilde{g} \in \mathbb{C}^N, \tilde{f} \in \mathbb{R} \times \mathbb{C}^{N-1}\}$ satisfying $\text{diag}(\tilde{g})\mathcal{H}(\tilde{f})\text{diag}(\tilde{g}) = \text{diag}(g)\mathcal{H}(f)\text{diag}(\bar{g})$, then there exists $c_0 > 0$ and $c_1, c_2 \in \mathbb{R}$ such that*

$$\tilde{g}_n = c_0 e^{i(c_1 + nc_2)} g_n, \quad \tilde{f}_n = c_0^{-2} e^{-inc_2} f_n, \quad n = 0, \dots, N-1.$$

Proof. We write $g_n = \alpha_n e^{i\beta_n}$ where α_n is the calibration amplitude and β_n is the calibration phase at the n th sensor. Then $\alpha = |g|$ and $\beta = \angle g$. Similarly, let $\tilde{\alpha} = |\tilde{g}|$ and $\tilde{\beta} = \angle \tilde{g}$. Observe that the diagonal entries of R^y are

$$R_{n,n}^y = \alpha_n^2 f_0, \quad n = 0, \dots, N-1.$$

If f_0 is given, then $\tilde{\alpha}_n = \sqrt{R_{n,n}^y / f_0}$; otherwise, the unknown f_0 leads to a scaling ambiguity such that $\tilde{\alpha} = c_0 \alpha$.

The sub-diagonal entries of R^y are

$$R_{n,n-1}^y = \alpha_n \alpha_{n-1} e^{i(\beta_n - \beta_{n-1})} f_1 \neq 0, \quad n = 1, \dots, N-1.$$

This gives rise to $N-2$ equations about the β_n 's:

$$e^{i(\beta_{n+1} - 2\beta_n + \beta_{n-1})} = \frac{\alpha_{n-1} R_{n+1,n}^y}{\alpha_{n+1} R_{n,n-1}^y},$$

which are equivalent to

$$\beta_{n+1} - 2\beta_n + \beta_{n-1} = \angle \frac{R_{n+1,n}^y}{R_{n,n-1}^y} + 2\pi k_n, \quad n = 1, \dots, N-2, \quad k_n \in \mathbb{Z}. \quad (13)$$

The linear system for β given by (13) has $N-2$ independent equations and N variables. Solving (13) results in

$$\tilde{\beta} = \beta + c_1 \begin{bmatrix} 1 \\ 1 \\ \vdots \\ 1 \\ 1 \end{bmatrix} + c_2 \begin{bmatrix} 0 \\ 1 \\ \vdots \\ N-2 \\ N-1 \end{bmatrix} \quad \text{mod } 2\pi.$$

Therefore, $\tilde{\beta}_n = \beta_n + c_1 + nc_2 \pmod{2\pi}$, which combined with $\tilde{\alpha} = c_0 \alpha$, results in $\tilde{g}_n = c_0 e^{i(c_1 + nc_2)} g_n$. As for \tilde{f} , since $R_{m,n}^y = g_m \bar{g}_n f_{m-n} = \tilde{g}_m \tilde{g}_n \tilde{f}_{m-n}$, we obtain $\tilde{f}_{m-n} = c_0^{-2} e^{-i(m-n)c_2} f_{m-n}$, which concludes the proof. \square

After obtaining the calibration parameters $\{\tilde{g}_n = c_0 e^{i(c_1 + nc_2)} g_n\}_{n=0}^{N-1}$, we simply divide \tilde{g} from R^y to obtain

$$\tilde{F} = \text{diag}(\tilde{g})^{-1} R^y \text{diag}(\tilde{g})^{-1} = c_0^{-2} D_{c_2} A R^x A^* D_{c_2}^* = c_0^{-2} \tilde{A} R^x \tilde{A}^*,$$

where $D_{c_2} = \text{diag} \left(\{e^{-inc_2}\}_{n=0}^{N-1} \right)$ and

$$\tilde{A}_{n,j} \in \mathbb{C}^{N \times s} : \tilde{A}_{n,j} = \frac{1}{\sqrt{N}} e^{2\pi i n (\omega_j - \frac{c_2}{2\pi})} \quad (14)$$

We can then perform standard spectral estimation on \tilde{F} to retrieve the frequencies. We consider the Multiple Signal Classification (MUSIC) algorithm proposed by Schmidt [22, 23]. We postpone the introduction of MUSIC to Section 3, and for now, we use the result that MUSIC guarantees an exact recovery of frequencies in the noiseless case as long as $N \geq s + 1$ (see Proposition 1). Combining Lemma 1 and exact recovery of MUSIC from noiseless data proves Theorem 1.

3 Algebraic methods

3.1 Full algebraic method and phase wrapping

In [19], Paulraj and Kailath propose the first method for sensor calibration in DOA estimation. By exploiting the Toeplitz structure of $\mathcal{H}(f)$, they obtain two linear systems in the calibration amplitudes and phases, respectively.

Consider the case with infinite snapshots of noiseless measurements. When k varies from 1 to $N - 1$, the k -th sub-diagonal entries of R^y satisfy

$$\alpha_{l+k} \alpha_l e^{i(\beta_{l+k} - \beta_l)} f_k = R_{l+k,l}^y, \quad l = 0, \dots, N - k - 1.$$

For $k = 1, \dots, N - 1$, as long as $|f_k| \neq 0$, then we can obtain the following system of equations in $\ln \alpha$

$$\ln \alpha_{l+k+1} + \ln \alpha_{l+1} - \ln \alpha_{l+k} - \ln \alpha_l = \ln \frac{|R_{l+k+1,l+1}^y|}{|R_{l+k,l}^y|} \quad (15)$$

together with (7) in β , for $l = 0, \dots, N - k - 2$. Paulraj and Kailath propose to substitute \equiv (equal modulo 2π) with $=$ in (7) and solve these linear systems by least squares. However, one has to consider phase wrapping in (7) so that (7) is equivalent to

$$\beta_{l+k+1} - \beta_{l+k} - \beta_{l+1} + \beta_l = \angle R_{l+k+1,l+1}^y / R_{l+k,l}^y + 2\pi p_{k,l} \text{ where } p_{k,l} \in \mathbb{Z} \quad (16)$$

where $l = 0, \dots, N - k - 2$ and $k = 1, \dots, N - 1$. Importantly, the $p_{k,l}$'s in (16) are not independent. For example, the parameters $p_{1,0}, p_{1,1}, p_{2,0}$ need to satisfy

$$\angle R_{2,1}^y / R_{1,0}^y + 2\pi p_{1,0} + \angle R_{3,2}^y / R_{2,1}^y + 2\pi p_{1,1} = \angle R_{3,1}^y / R_{2,0}^y + 2\pi p_{2,0}. \quad (17)$$

The $p_{k,l}$'s are constrained by many more equations like (17). Solving (16) with those constraints involves phase synchronization, which itself is highly nontrivial.

3.2 Partial algebraic method

In [31], Wylie, Roy and Schmitt proposed a partial algebraic method by using the part of equations in (7) with $k = 1$ to recover the calibration phases. These linear equations are independent so there is no problem of phase wrapping any more. This partial algebraic method is summarized in Algorithm 1.

Algorithm 1 Partial algebraic method

Input: Measurements $\{y_e(t), t \in \Gamma\}$ and sparsity s

Output: Calibration parameters $\hat{g} = \{\hat{g}_n := \hat{\alpha}_n e^{i\hat{\beta}_n}\}_{n=0}^{N-1}$ and recovered spectrum $\{\hat{\omega}_j\}_{j=1}^s$

- 1: Form the empirical covariance matrix $\tilde{R}_e^y = 1/L \sum_{t \in \Gamma} y_e(t) y_e^*(t)$
- 2: Compute the eigenvalue decomposition:

$$\tilde{R}_e^y = U \Sigma U^*$$

where

$$\Sigma = \text{diag}(\lambda_0(\tilde{R}_e^y), \dots, \lambda_{N-1}(\tilde{R}_e^y)), \lambda_0(\tilde{R}_e^y) \geq \lambda_1(\tilde{R}_e^y) \geq \dots$$

- 3: Estimate the noise level $\hat{\sigma} = \sqrt{\sum_{l=s}^{N-1} \lambda_l(\tilde{R}_e^y) / (N - s)}$

- 4: Subtract the noise component: $\tilde{R}^y \leftarrow \tilde{R}_e^y - \hat{\sigma}^2 I_N$

- 5: $\hat{\alpha}_n = \sqrt{\hat{R}_{n,n}^y}$, $n = 0, \dots, N - 1$

- 6: Solve the following linear system $\Phi \beta = R$ to obtain calibration phases $\hat{\beta}$

$$\underbrace{\begin{bmatrix} \frac{1}{N^2} & 0 & 0 & 0 & \dots & 0 & 0 & 0 \\ 1 & -2 & 1 & 0 & \dots & 0 & 0 & 0 \\ 0 & 1 & -2 & 1 & \dots & 0 & 0 & 0 \\ & & & \dots & & & & \\ & & & \dots & & & & \\ & & & \dots & & & & \\ 0 & 0 & 0 & 0 & \dots & 1 & -2 & 1 \\ 0 & 0 & 0 & 0 & \dots & 0 & 0 & \frac{1}{N^2} \end{bmatrix}}_{\Phi \in \mathbb{R}^{N \times N}} \underbrace{\begin{bmatrix} \beta_0 \\ \beta_1 \\ \beta_2 \\ \vdots \\ \beta_{N-3} \\ \beta_{N-2} \\ \beta_{N-1} \end{bmatrix}}_{\beta \in \mathbb{R}^N} = \underbrace{\begin{bmatrix} 0 \\ \angle(R_{2,1}^y/R_{1,0}^y) \\ \angle(R_{3,2}^y/R_{2,1}^y) \\ \vdots \\ \vdots \\ \vdots \\ \angle(R_{N-1,N-2}^y/R_{N-2,N-1}^y) \\ 0 \end{bmatrix}}_{b \in \mathbb{R}^N} \quad (18)$$

- 7: Compute the matrix $\hat{F} = \hat{G}^{-1} \tilde{R}^y \hat{G}^{-1}$ where $\hat{G} = \text{diag}(\hat{g})$ and $\hat{g}_n = \hat{\alpha}_n e^{i\hat{\beta}_n}$, $n = 0, \dots, N - 1$

- 8: Apply the MUSIC algorithm on \hat{F} :

- i) Compute the eigenvalue decomposition:

$$\hat{F} = [V_1 \ V_2] \text{diag}(\lambda_1(\hat{F}), \dots, \lambda_s(\hat{F}), \dots) [V_1 \ V_2]^*$$

where $V_1 \in \mathbb{C}^{N \times s}$, and $\lambda_1(\hat{F}) \geq \lambda_2(\hat{F}) \geq \dots$

- ii) Compute the imaging function

$$\hat{\mathcal{J}}(\omega) = \frac{\|\phi(\omega)\|}{\|V_2^* \phi(\omega)\|}$$

where $\phi(\omega) = [1 \ e^{2\pi i \omega} \ \dots \ e^{2\pi i(N-1)\omega}]^T$

- iii) Return the spectrum $\{\hat{\omega}_j\}_{j=1}^s$ corresponding to the s largest local maxima of $\hat{\mathcal{J}}(\omega)$
-

In practice, we take L snapshots of independent measurements, i.e., $\{y_e(t), t \in \Gamma, \#\Gamma = L\}$,

and approximate R_e^y by the empirical covariance matrix

$$\tilde{R}_e^y = \frac{1}{L} \sum_{t \in \Gamma} y_e(t) y_e^*(t).$$

We first estimate the noise level σ from the smallest $N - s$ eigenvalues of \tilde{R}_e^y and then subtract the noise component from \tilde{R}_e^y to obtain \hat{R}^y as an approximation of R^y (see Step 4 in Algorithm 1). We then identify the calibration amplitudes $|g|$ from the diagonal R^y and calibration phases $\angle g$ from the sub-diagonal R^y by solving (18) which gives a specific solution to (13) with $\beta_0 = \beta_{N-1} = 0$. After the calibration parameters are recovered, we apply the MUSIC algorithm for the usual spectral estimation, where exact recovery is guaranteed in the noiseless case.

Proposition 1. *Suppose s is known and the input of MUSIC is exact: $F = AR^x A^*$. If $N \geq s + 1$, then*

$$\omega \in \mathcal{S} \iff \mathcal{R}(\omega) = 0 \iff \mathcal{J}(\omega) = \infty$$

where $\mathcal{J}(\omega)$ is the imaging function defined in Step 8.ii in Algorithm 1 and $\mathcal{R}(\omega) := 1/\mathcal{J}(\omega)$ is called the noise-space correlation function.

In the noiseless case, one simply needs to extract s zeros of the noise-space correlation function $\mathcal{R}(\omega)$, or the s largest local maxima of the imaging function $\mathcal{J}(\omega)$ as a recovery of \mathcal{S} . In the presence of noise, we assume the input of MUSIC is approximate: $\hat{F} = AR^x A^* + E$. Then the noise-space correlation function is perturbed from \mathcal{R} to $\hat{\mathcal{R}}$ with an upper bound given below.

Proposition 2 ([15, Theorem 3]). *Let $N \geq s + 1$. Suppose s is known and the input of MUSIC is approximate: $\hat{F} = F + E = AR^x A^* + E$. Let $\mathcal{R}(\omega)$ and $\hat{\mathcal{R}}(\omega)$ be the imaging functions when MUSIC is applied on F and \hat{F} respectively. Then*

$$\sup_{\omega \in [0,1]} |\hat{\mathcal{R}}(\omega) - \mathcal{R}(\omega)| \leq \frac{4\lambda_1(F) + 2\|E\|}{(\lambda_s(F) - \|E\|)^2} \|E\|$$

where $\lambda_1(F) \geq \dots \geq \lambda_s(F)$ are the nonzero eigenvalues of F .

3.3 Sensitivity of the partial algebraic method

Theorem 1 guarantees exact recovery up to a trivial ambiguity with infinite snapshots of noiseless measurements. In practice, only finite snapshots of noisy measurements are taken. We next present a sensitivity analysis of the partial algebraic method in Algorithm 1 with respect to the number of snapshots L and noise level σ . We prove that, there exist $C_1, C_2 > 0$ such that

$$\text{Reconstruction error of calibration parameters} \leq O\left(\frac{C_1 + C_2 \max(\sigma, \sigma^2)}{\sqrt{L}}\right)$$

by the partial algebraic method when the true frequencies are separated by $1/N$. As for frequency localization in the MUSIC algorithm, the recovered frequencies correspond to the smallest local minima of the noise-space correlation function. We prove that, the noise-space correlation function is perturbed by infinite snapshots and noise at most by $O\left(\frac{C_3 + C_4 \max(\sigma, \sigma^2)}{\sqrt{L}}\right)$ for some constants $C_3, C_4 > 0$.

In the theorem below, let $\gamma_{\max} = \max_j \gamma_j$, $\gamma_{\min} = \min_j \gamma_j$, and $\alpha_{\max} = \max_n |g_n|$, $\alpha_{\min} = \min_n |g_n|$.

Theorem 2. Assume $N \geq s + 1$ and $|f_1| > 0$. Suppose we apply the partial algebraic method in Algorithm 1 with L snapshots of independent measurements. Let \widehat{R}^y be the outcome in Step 4, \widehat{g} be the recovered calibration parameters, and \widehat{F} be the outcome in Step 7. Define

$$\begin{aligned} \Delta R^y &:= 2\alpha_{\max}^2 \sigma_{\max}^2(A) \left(\frac{\gamma_{\max} \max_t \|x(t)\| \sqrt{2 \log 4s}}{\sqrt{L}} + \frac{\gamma_{\max}^2 + \max_{t \in \Gamma} \|x(t)\|^2}{3L} \log 4s \right) \\ &+ 4\alpha_{\max} \sigma_{\max}(A) \left(\frac{\sigma \gamma_{\max} \sqrt{2N \log(N+s)}}{\sqrt{L}} + \frac{\max_{t \in \Gamma} \|x(t)\| \|e(t)\|}{3L} \log(N+s) \right) \\ &+ 2 \left(\frac{\sigma \max_t \|e(t)\| \sqrt{2 \log 2N}}{\sqrt{L}} + \frac{\sigma^2 + \max_{t \in \Gamma} \|e(t)\|^2}{3L} \log 2N \right). \end{aligned} \quad (19)$$

Then $\mathbb{E} \|R^y - \widehat{R}^y\| \leq \Delta R^y$, and

$$\mathbb{E} \min_{c_0 > 0, c_1, c_2 \in \mathbb{R}} \max_n \|c_0 \widehat{g}_n - e^{i(c_1 + nc_2)} g_n\|_{\infty} \leq \left(\frac{3(\|g\|^2 + N\alpha_{\max}^2)}{2\alpha_{\min} \|g\|^2 f_0} + 144N^2 \frac{\alpha_{\max}^5}{\alpha_{\min}^6 |f_1|^2} \right) \Delta R^y \quad (20)$$

$$\mathbb{E} \min_{c_2 \in \mathbb{R}} \sup_{\omega \in [0, 1)} \left| \widehat{\mathcal{R}}(\omega) - \mathcal{R}\left(\omega - \frac{c_2}{2\pi}\right) \right| \leq \frac{4\lambda_1(F) + 2\Delta F}{(\lambda_s(F) - \Delta F)^2} \Delta F \quad (21)$$

where $F = AR^x A^*$, $\mathcal{R}(\omega)$ and $\widehat{\mathcal{R}}(\omega)$ are the noise-space correlation functions in MUSIC with input data F and \widehat{F} respectively, and

$$\Delta F = \left[\frac{9}{\alpha_{\min}^2} + \frac{12\alpha_{\max}^2 \gamma_{\max}^2 \sigma_{\max}^2(A)}{\alpha_{\min}^3} \left(\frac{3(\|g\|^2 + N\alpha_{\max}^2)}{2\alpha_{\min} \|g\|^2 f_0} + \frac{144N^2 \alpha_{\max}^5}{\alpha_{\min}^6 |f_1|^2} \right) \right] \Delta R^y.$$

The expectations in (20) and (21) are taken over random source amplitudes and random noises. To get some intuition, our estimates suggest that, the partial algebraic method is more stable in the cases where 1) the noise level σ is small and the number of snapshots L is large; 2) $\|g\|$, f_0 , $|f_1|$ are large; 3) the calibration parameters g have a small dynamic range such that $\alpha_{\max}/\alpha_{\min} \approx 1$; 4) the minimal calibration amplitude α_{\min} is large; 5) source amplitudes have a small dynamic range such that $\gamma_{\max}/\gamma_{\min} \approx 1$; 6) frequencies are well separated such that $\sigma_{\max}(A)/\sigma_{\min}(A) \approx 1$.

Notice that $\mathbb{E} \|x(t)\| = \sqrt{\sum_{j=1}^s \gamma_j^2}$ and $\mathbb{E} \|e(t)\| = \sigma \sqrt{N}$. Suppose $\|x(t)\|$ and $\|e(t)\|$ concentrate around $\mathbb{E} \|x(t)\|$ and $\mathbb{E} \|e(t)\|$ respectively. In the case that the true frequencies in \mathcal{S} are separated by $q > 1/N$, discrete Ingham inequalities [15, Theorem 2] guarantee that $r_1(q, N) \leq \sigma_{\min}(A) \leq \sigma_{\max}(A) \leq r_2(q, N)$ for some positive constants r_1, r_2 depending on q, N , which implies $\lambda_1(F) \leq \gamma_{\max}^2 r_2^2$ and $\lambda_s(F) \geq \gamma_{\min}^2 r_1^2$. Then, when L is sufficiently large, we have

$$\Delta R^y \leq O \left(\frac{c_1 + c_2 \max(\sigma, \sigma^2)}{\sqrt{L}} \right)$$

for some positive constants c_1, c_2 depending on $g, \{\gamma_j\}_{j=1}^s, \mathcal{S}, N, s$. Therefore

$$\begin{aligned} \mathbb{E} \min_{c_0 > 0, c_1, c_2 \in \mathbb{R}} \max_n \|c_0 \widehat{g}_n - e^{i(c_1 + nc_2)} g_n\|_{\infty} &\leq O \left(\frac{C_1 + C_2 \max(\sigma, \sigma^2)}{\sqrt{L}} \right) \\ \mathbb{E} \min_{c_2 \in \mathbb{R}} \sup_{\omega \in [0, 1)} \left| \widehat{\mathcal{R}}(\omega) - \mathcal{R}\left(\omega - \frac{c_2}{2\pi}\right) \right| &\leq O \left(\frac{C_3 + C_4 \max(\sigma, \sigma^2)}{\sqrt{L}} \right) \end{aligned}$$

for some positive constants C_1, C_2, C_3, C_4 depending on $g, \{\gamma_j\}_{j=1}^s, \mathcal{S}, N, s$.

Theorem 2 is related to the analysis in [13]. Suppose the problem of phase wrapping in the full algebraic method can be resolved. In [13], Li and Er split the reconstruction errors of the

calibration amplitudes and phases to an average bias term and a variance term. They claim that the average bias is nonzero, and the variance for the calibration phases is $O(1/\sqrt{L})$ where L is the number of snapshots. Below we point out some differences between Theorem 2 and the analysis in [13].

1. In [13] the authors claim that the average bias is non-zero. In this case the total reconstruction error for the calibration phases does not approach 0 as $L \rightarrow \infty$. In comparison, we show that the reconstruction error of the calibration parameters and the perturbation of the noise-space correlation function in MUSIC converge to 0 as $L \rightarrow \infty$ in Theorem 2.
2. We present a sensitivity analysis of the partial algebraic method to both the number of snapshots and noise, while sensitivity to noise is not addressed in [13].
3. The upper bounds in Theorem 2 are explicitly given in terms of g , $\{\gamma_j\}_{j=1}^s$, N , s , $\sigma_{\max}(A)$ and $\sigma_{\min}(A)$. When the underlying frequencies are separated by $q > 1/N$, we can further bound $\sigma_{\max}(A)$ and $\sigma_{\min}(A)$ in terms of q and N by discrete Ingham inequalities [15]. In comparison, all bounds in [13] are implicit in the sense that the average bias is defined but not analyzed, and the variance is expressed in terms of the trace of certain matrices that are not explicitly given.
4. One needs to perform standard spectral estimation after calibration parameters are recovered. Theorem 2 includes a sensitivity analysis of the MUSIC algorithm, which is not addressed in [13].

In Theorem 2, the expression in (19) may appear intimidating. However, it simply results from Bernstein inequalities [28], based on which we estimate the deviation of the sampled covariance matrix \hat{R}_e^y from the covariance matrix R_e^y . Notice that

$$\begin{aligned} \|\hat{R}_e^y - R_e^y\| &\leq \|GA(R^x - \tilde{R}^x)A^*G^* + GA(R^{xe} - \tilde{R}^{xe}) + (R^{ex} - \tilde{R}^{ex})A^*G^* + R^e - \tilde{R}^e\| \\ &\leq \sigma_{\max}^2(G)\sigma_{\max}^2(A)\|R^x - \tilde{R}^x\| + \sigma_{\max}(G)\sigma_{\max}(A)\|R^{xe} - \tilde{R}^{xe}\| \\ &\quad + \sigma_{\max}(G)\sigma_{\max}(A)\|R^{ex} - \tilde{R}^{ex}\| + \|R^e - \tilde{R}^e\|. \end{aligned}$$

Applying Bernstein inequalities gives rise to (19) where the three terms correspond to upper bounds of $\sigma_{\max}^2(G)\sigma_{\max}^2(A)\mathbb{E}\|R^x - \tilde{R}^x\|$, $\sigma_{\max}(G)\sigma_{\max}(A)\left(\mathbb{E}\|R^{xe} - \tilde{R}^{xe}\| + \mathbb{E}\|R^{ex} - \tilde{R}^{ex}\|\right)$, and $\mathbb{E}\|R^e - \tilde{R}^e\|$, respectively.

4 Optimization approach

As discussed in Section 3.1, it is nontrivial to make use of all entries in the covariance matrix in the algebraic method. Instead we propose an optimization approach to take advantage of all measurements.

Suppose \hat{R}^y is an estimate of R^y . According to Lemma 1, we can recover exact calibration parameters g and the quantities defined in (6), denoted by f , by solving the following optimization problem:

$$\min_{\mathbf{g}, \mathbf{f} \in \mathbb{C}^N} \mathcal{L}(\mathbf{g}, \mathbf{f}) := \left\| \text{diag}(\mathbf{g})\mathcal{H}(\mathbf{f})\text{diag}(\bar{\mathbf{g}}) - \hat{R}^y \right\|_F^2. \quad (22)$$

Here we use boldface letters \mathbf{g}, \mathbf{f} to denote variables in optimization and g, f to denote the ground truth. With infinite snapshots of noiseless measurements, we have $\hat{R}^y = R^y$, and

Lemma 1 indicates that the global minimizer of (22) is the ground truth. Otherwise, we run Step 1 - 4 in Algorithm 2 to obtain \widehat{R}^y as an approximation to R^y .

As pointed out in Lemma 1, if (\mathbf{g}, \mathbf{f}) is a solution to (22), then so is $(c_0\mathbf{g}, c_0^{-2}\mathbf{f})$ for any $c_0 \neq 0$. In order to guarantee numerical stability, we avoid the case that $\|\mathbf{g}\| \rightarrow 0$ and $\|\mathbf{f}\| \rightarrow \infty$ (or vice versa) by adding a penalty to the objective function. Let $n_0 := \|g\|^2\|f\|$ which can be estimated from \widehat{R}^y based on the following lemma (see Appendix B for the proof):

Lemma 2. *Let R^y be defined in (9). Then*

$$n_0 = \left(\sum_{n=0}^{N-1} R_{n,n}^y \right) \sqrt{1 + \frac{1}{N-k} \sum_{k=1}^{N-1} \sum_{n=0}^{N-k-1} \frac{|R_{n+k,n}^y|^2}{R_{n+k,n+k}^y R_{n,n}^y}}. \quad (23)$$

Let \widehat{n}_0 be the estimate of n_0 from Step 5 in Algorithm 2. Theorem 2 shows that $\|\widehat{R}^y - R^y\| \leq \Delta R^y$ with ΔR^y given by (19). When the true frequencies are separated by $1/N$, $\Delta R^y \leq O\left(\frac{c_1+c_2 \max(\sigma, \sigma^2)}{\sqrt{L}}\right)$, which implies $\widehat{n}_0 \approx n_0$ when L is sufficiently large.

Consider the following bounded set:

$$\mathcal{N}_{\widehat{n}_0} = \{(\mathbf{g}, \mathbf{f}) : \|\mathbf{g}\|^2 \leq 2\sqrt{\widehat{n}_0}, \|\mathbf{f}\| \leq 2\sqrt{\widehat{n}_0}\}. \quad (24)$$

We pick an initial point satisfying

$$(\mathbf{g}^0, \mathbf{f}^0) : \|\mathbf{g}^0\|^2 \leq \sqrt{2\widehat{n}_0}, \|\mathbf{f}^0\| \leq \sqrt{2\widehat{n}_0}. \quad (25)$$

through the partial algebraic method. Notice that the solution from the partial algebraic method has a scaling ambiguity, so we simply normalize it to guarantee (25). In order to ensure all the iterates remain in $\mathcal{N}_{\widehat{n}_0}$, we minimize the following regularized function:

$$\min_{\mathbf{g}, \mathbf{f} \in \mathbb{C}^N} \tilde{\mathcal{L}}(\mathbf{g}, \mathbf{f}) := \mathcal{L}(\mathbf{g}, \mathbf{f}) + \mathcal{G}(\mathbf{g}, \mathbf{f}) \quad (26)$$

where $\mathcal{L}(\mathbf{g}, \mathbf{f})$ is defined in (22) and $\mathcal{G}(\mathbf{g}, \mathbf{f})$ is a penalty function of the form

$$\mathcal{G}(\mathbf{g}, \mathbf{f}) = \rho \left[\mathcal{G}_0 \left(\frac{\|\mathbf{f}\|^2}{2\widehat{n}_0} \right) + \mathcal{G}_0 \left(\frac{\|\mathbf{g}\|^2}{\sqrt{2\widehat{n}_0}} \right) \right]$$

where $\mathcal{G}_0(z) = (\max(z-1, 0))^2$ and $\rho \geq \frac{3\widehat{n}_0 + \|R^y - \widehat{R}^y\|_F}{(\sqrt{2}-1)^2}$. When exact frequencies are separated by $1/N$, we have $\|\widehat{R}^y - R^y\| = O\left(\frac{c_1+c_2 \max(\sigma, \sigma^2)}{\sqrt{L}}\right)$. It follows that $\|\widehat{R}^y - R^y\|_F \leq \sqrt{N}\|\widehat{R}^y - R^y\| \leq \sqrt{N}\Delta R^y \rightarrow 0$ as $L \rightarrow \infty$. We therefore take $\rho \geq 3\widehat{n}_0/(\sqrt{2}-1)^2$ when L is sufficiently large.

The objective function in (26) is continuously differentiable but non-convex. We pick a random initial point satisfying (25) and solve (26) by gradient descent where the derivative can be interpreted as Wirtinger derivative¹. Here the Wirtinger gradient of $\tilde{\mathcal{L}}$ is

$$\nabla \tilde{\mathcal{L}} = \left[\nabla_{\mathbf{g}} \tilde{\mathcal{L}} \quad \nabla_{\mathbf{f}} \tilde{\mathcal{L}} \right]^T = \left[\nabla_{\mathbf{g}} \mathcal{L} + \nabla_{\mathbf{g}} \mathcal{G} \quad \nabla_{\mathbf{f}} \mathcal{L} + \nabla_{\mathbf{f}} \mathcal{G} \right]^T$$

¹Let $z = x + iy$ and $h(z) = h(x, y) = u(x, y) + iv(x, y)$. The Wirtinger derivatives and gradient of h is

$$\frac{\partial h}{\partial z} := \frac{1}{2} \left(\frac{\partial h}{\partial x} - i \frac{\partial h}{\partial y} \right), \quad \nabla_z h := \frac{\partial h}{\partial \bar{z}} := \frac{1}{2} \left(\frac{\partial h}{\partial x} + i \frac{\partial h}{\partial y} \right).$$

Algorithm 2 Optimization approach

Input: Measurements $\{y_e(t), t \in \Gamma\}$ and sparsity s

Output: Calibration parameters $\hat{\mathbf{g}}$ and recovered spectrum $\{\hat{\omega}_j\}_{j=1}^s$

- 1: Form the empirical covariance matrix $\tilde{R}_e^y = 1/L \sum_{t \in \Gamma} y_e(t) y_e^*(t)$
- 2: Compute the eigenvalue decomposition: $\tilde{R}_e^y = U \Sigma U^*$ where $\Sigma = \text{diag}(\lambda_0(\tilde{R}_e^y), \dots, \lambda_{N-1}(\tilde{R}_e^y))$, $\lambda_0(\tilde{R}_e^y) \geq \lambda_1(\tilde{R}_e^y) \geq \dots$
- 3: Estimate the noise level $\hat{\sigma} = \sqrt{\sum_{l=s}^{N-1} \lambda_l(\tilde{R}_e^y) / (N-s)}$
- 4: Subtract the noise component: $\tilde{R}^y \leftarrow \tilde{R}_e^y - \hat{\sigma}^2 I_N$
- 5: Compute

$$\hat{n}_0 = \sum_{n=0}^{N-1} \hat{R}_{n,n}^y \sqrt{1 + \frac{1}{N-k} \sum_{k=1}^{N-1} \sum_{n=0}^{N-k-1} \frac{|\hat{R}_{n+k,n}^y|^2}{\hat{R}_{n+k,n+k}^y \hat{R}_{n,n}^y}}.$$

6: Initialization:

- (i) Run Step 1 - 7 in Algorithm 1, and let $\mathbf{g}^0 \leftarrow \hat{\mathbf{g}}$ and $F^0 \leftarrow \hat{F}$
- (ii) Let $\mathbf{f}^0 \in \mathbb{C}^N$ such that $\mathbf{f}_k^0 = \frac{1}{N-k} \sum \text{diag}(F^0, -k)$, $k = 0, \dots, N-1$
- (iii) $\mathbf{g}^0 \leftarrow \sqrt[4]{\hat{n}_0} \frac{\mathbf{g}^0}{\|\mathbf{g}^0\|}$ and $\mathbf{f}^0 \leftarrow \sqrt{\hat{n}_0} \frac{\mathbf{f}^0}{\|\mathbf{f}^0\|}$
- 7: **for** $k = 1, 2, \dots$, **do**
- 8: $\mathbf{g}^k = \mathbf{g}^{k-1} - \eta^k \nabla_{\mathbf{g}} \tilde{\mathcal{L}}(\mathbf{g}^{k-1}, \mathbf{f}^{k-1})$
- 9: $\mathbf{f}^k = \mathbf{f}^{k-1} - \eta^k \nabla_{\mathbf{f}} \tilde{\mathcal{L}}(\mathbf{g}^{k-1}, \mathbf{f}^{k-1})$
- 10: **end for**
- 11: Output of gradient descent: $\hat{\mathbf{g}}$ and $\hat{\mathbf{f}}$
- 12: Apply MUSIC to $\mathcal{H}(\hat{\mathbf{f}})$:

- i) Compute the eigenvalue decomposition:

$$\mathcal{H}(\hat{\mathbf{f}}) = [V_1 \ V_2] \text{diag}(\lambda_1(\mathcal{H}(\hat{\mathbf{f}})), \dots, \lambda_s(\mathcal{H}(\hat{\mathbf{f}})), \dots) [V_1 \ V_2]^*$$

where $V_1 \in \mathbb{C}^{N \times s}$, and $\lambda_1(\mathcal{H}(\hat{\mathbf{f}})) \geq \lambda_2(\mathcal{H}(\hat{\mathbf{f}})) \geq \dots$

- ii) Compute the imaging function

$$\hat{\mathcal{J}}(\omega) = \frac{\|\phi(\omega)\|}{\|V_2^* \phi(\omega)\|}$$

where $\phi(\omega) = [1 \ e^{2\pi i \omega} \ \dots \ e^{2\pi i (N-1)\omega}]^T$

- iii) Return the spectrum $\{\hat{\omega}_j\}_{j=1}^s$ corresponding to the s largest local maxima of $\hat{\mathcal{J}}(\omega)$
-

with each term given by

$$\nabla_{\mathbf{g}} \mathcal{L} = 2 \text{diag} \left[\overline{\mathcal{H}(\mathbf{f})^* \text{diag}(\bar{\mathbf{g}}) \left(\text{diag}(\mathbf{g}) \mathcal{H}(\mathbf{f}) \text{diag}(\bar{\mathbf{g}}) - \hat{R}^y \right)} \right], \quad (27)$$

$$\nabla_{\mathbf{f}} \mathcal{L} = \mathcal{H}^a \left[\text{diag}(\bar{\mathbf{g}}) \left(\text{diag}(\mathbf{g}) \mathcal{H}(\mathbf{f}) \text{diag}(\bar{\mathbf{g}}) - \hat{R}^y \right) \text{diag}(\mathbf{g}) \right], \quad (28)$$

$$\nabla_{\mathbf{g}} \mathcal{G} = \frac{\rho}{\sqrt{2\hat{n}_0}} \mathcal{G}'_0 \left(\frac{\|\mathbf{g}\|^2}{\sqrt{2\hat{n}_0}} \right) \mathbf{g},$$

$$\nabla_{\mathbf{f}} \mathcal{G} = \frac{\rho}{2\hat{n}_0} \mathcal{G}'_0 \left(\frac{\|\mathbf{f}\|^2}{2\hat{n}_0} \right) \mathbf{f},$$

where $\mathcal{G}'_0(z) = 2 \max(z - 1, 0)$. The operator $\mathcal{H}^a : \mathbb{C}^{N \times N} \rightarrow \mathbb{C}^N$ is associated with \mathcal{H} and defined by

$$\mathcal{H}^a : \mathbb{C}^{N \times N} \rightarrow \mathbb{C}^N : \mathcal{H}^a(X) = \begin{bmatrix} \sum (\text{diag}(X) + \text{diag}(\bar{X})) \\ \sum (\text{diag}(X, 1) + \text{diag}(\bar{X}, -1)) \\ \vdots \\ \sum (\text{diag}(X, N-1) + \text{diag}(\bar{X}, -(N-1))) \end{bmatrix}.$$

One can verify that \mathcal{H}^a satisfies

$$\frac{\partial}{\partial \mathbf{f}} \left(\langle \mathcal{H}(\mathbf{f}), X \rangle + \langle X, \mathcal{H}(\mathbf{f}) \rangle \right) = \mathcal{H}^a(X), \quad \forall X \in \mathbb{C}^{N \times N},$$

and therefore

$$\begin{aligned} \frac{\partial \mathcal{L}}{\partial \mathbf{f}} &= \frac{\partial}{\partial \mathbf{f}} \left(\left\langle \mathcal{H}(\mathbf{f}), \text{diag}(\bar{\mathbf{g}}) \left(\text{diag}(\mathbf{g}) \mathcal{H}(\mathbf{f}) \text{diag}(\bar{\mathbf{g}}) - \hat{R}^y \right) \text{diag}(\mathbf{g}) \right\rangle \right. \\ &\quad \left. + \left\langle \text{diag}(\bar{\mathbf{g}}) \left(\text{diag}(\mathbf{g}) \mathcal{H}(\mathbf{f}) \text{diag}(\bar{\mathbf{g}}) - \hat{R}^y \right) \text{diag}(\mathbf{g}), \mathcal{H}(\mathbf{f}) \right\rangle \right) \\ &= \mathcal{H}^a \left[\text{diag}(\bar{\mathbf{g}}) \left(\text{diag}(\mathbf{g}) \mathcal{H}(\mathbf{f}) \text{diag}(\bar{\mathbf{g}}) - \hat{R}^y \right) \text{diag}(\mathbf{g}) \right] \end{aligned}$$

which gives rise to (28).

Our approach is summarized in Algorithm 2. The next theorem proves that the gradient descent in Step 6-11 of Algorithm 2 converges to a critical point of (26).

Theorem 3. *Let (g, f) be the ground truth. Let \hat{R}^y be an estimate of R^y . Assume that the initialization $(\mathbf{g}^0, \mathbf{f}^0)$ satisfies $\|\mathbf{g}^0\| \leq \sqrt[4]{2\hat{n}_0}$ and $\|\mathbf{f}^0\| \leq \sqrt{2\hat{n}_0}$, and $\rho \geq \frac{3\hat{n}_0 + \|R^y - \hat{R}^y\|_F}{(\sqrt{2}-1)^2}$. Then running Algorithm 2 with step size*

$$\eta^k \leq 2/C_{\text{Lip}} \tag{29}$$

where

$$C_{\text{Lip}} \leq 166\hat{n}_0 \max(\sqrt{\hat{n}_0}, \sqrt[4]{\hat{n}_0}) + 8\hat{n}_0 + 16 \max(\sqrt{\hat{n}_0}, \sqrt[4]{\hat{n}_0}) \|R^y - \hat{R}^y\|_F + \frac{12\rho}{\min(\hat{n}_0, \sqrt{\hat{n}_0})}$$

gives rise to a sequence $(\mathbf{g}^k, \mathbf{f}^k) \in \mathcal{N}_{\hat{n}_0}$, and

$$\|\nabla \tilde{\mathcal{L}}(\mathbf{g}^k, \mathbf{f}^k)\| \rightarrow 0, \quad \text{as } k \rightarrow \infty.$$

Theorem 3 (see Appendix C for the proof) shows that Wirtinger gradient descent converges to a critical point of (26). Our numerical experiments suggest that this point provides a good approximation of the ground truth up to a trivial ambiguity.

5 Numerical experiments

We perform systematic numerical simulations to compare the performance of several methods. In our simulations, \mathcal{S} contains s frequencies located on the continuous domain $[0, 1)$. Theorem 2 shows that the problem is more challenging when the dynamic ranges of x and g increase. We denote the dynamic range of γ and g by $\text{DR}_\gamma > 0$ and $\text{DR}_g > 0$ respectively, such that $\gamma_i = (\mathbb{E}x_i^2(t))^{\frac{1}{2}} \in [1, \text{DR}_\gamma]$, $i = 1, \dots, s$ and $|g_i| \in [1, \text{DR}_g]$, $i = 0, \dots, N-1$. The phases of $x_j(t)$ are randomly chosen from $[0, 2\pi)$ to guarantee that $\mathbb{E}x(t)x^*(t) = \text{diag}(\{\gamma_i^2\}_{i=1}^s)$. We add i.i.d. Gaussian noise to the measurements such that $y_e(t) = y(t) + e(t)$ with $e(t) \sim \mathcal{N}(0, \sigma^2 I_N)$.

Suppose we take L snapshots of independent measurements, i.e., $\{y_e(t) : t = 1, \dots, L\}$, and form the empirical covariance matrix $\tilde{R}_e^y = \frac{1}{L} \sum_{t=1}^L y_e(t)y_e^*(t)$. We assume s is known and denote the support of recovered frequencies by $\hat{\mathcal{S}} = \{\hat{\omega}_j\}_{j=1}^s$. Due to discrete set-up of sensors, we assume periodicity of the frequency domain $[0, 1)$ on which the distance between two frequencies $d(\omega_j, \omega_l)$ is understood as the wrap-around distance on the torus. Frequency support error is measured by the Hausdorff distance between \mathcal{S} and $\hat{\mathcal{S}}$ up to a translation:

$$\text{SuppError} = d(\mathcal{S}, \hat{\mathcal{S}}) = \min_{c_2 \in [0, 2\pi)} \max \left(\max_{\hat{\omega} \in \hat{\mathcal{S}}} \min_{\omega \in \mathcal{S}} d \left(\hat{\omega} + \frac{c_2}{2\pi}, \omega \right), \max_{\omega \in \mathcal{S}} \min_{\hat{\omega} \in \hat{\mathcal{S}}} d \left(\hat{\omega} + \frac{c_2}{2\pi}, \omega \right) \right). \quad (30)$$

Let c_2^* be the argmin in (30). In the noiseless case, we expect the recovered calibration parameters in the form of $\hat{g}_n = c_0 e^{ic_1} e^{inc_2^*} g_n$ for some $c_0 > 0$ and $c_1 \in [0, 2\pi)$. Let $\tilde{g}_n = \hat{g}_n e^{-inc_2^*}$ and $C^* = \text{argmin}_C \sum_{n=0}^{N-1} |\tilde{g}_n - Cg_n|^2$. We measure the relative calibration error for the n -th sensor and the average relative calibration error as

$$\text{CalError}_n = \frac{|\tilde{g}_n - C^*g_n|}{|g_n|}, \quad \text{CalError} = \frac{1}{N} \sum_{n=0}^{N-1} \text{CalError}_n.$$

We test the following methods

- the partial algebraic method in Algorithm 1;
- the optimization approach in Algorithm 2: In practice we choose the step length η^k according to the backtracking line search in Algorithm 3 [18, Algorithm 3.1 on Page 37]. This backtracking approach ensures the selected step length η_k is short enough to guarantee a sufficient decrease of $\tilde{\mathcal{L}}$ but not too short. The latter claim holds since the accepted step length η_k is within a factor θ of the previous trial value η^k/θ , which was rejected for violating the sufficient decreases of $\tilde{\mathcal{L}}$, that is, for being too long. In our implementation, we set $\bar{\eta} = \tilde{\mathcal{L}}(\mathbf{g}^k, \mathbf{f}^k) / \|\nabla \tilde{\mathcal{L}}(\mathbf{g}^k, \mathbf{f}^k)\|$, $\theta = 0.5, c = 0.5$ and terminate gradient descent while $\eta^k < 10^{-4}$;

Algorithm 3 Backtracking line search

1: Choose $\bar{\eta} > 0, \theta \in (0, 1), c \in (0, 1)$; Set $\eta \leftarrow \bar{\eta}$; Denote $\mathbf{z}^k = (\mathbf{g}^k, \mathbf{f}^k)$ and $\mathbf{p}_k = -\nabla \tilde{\mathcal{L}}(\mathbf{g}^k, \mathbf{f}^k)$.

2: **repeat**

3: $\eta \leftarrow \theta\eta$

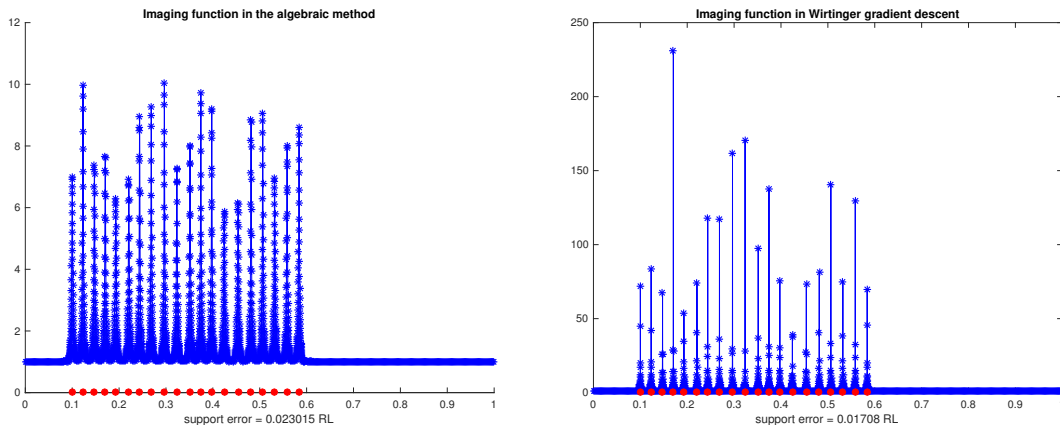
4: **until** $\mathcal{L}(\mathbf{z}_k + \eta\mathbf{p}_k) \leq \mathcal{L}(\mathbf{z}_k) - c\eta\|\mathbf{p}_k\|^2$.

5: **return** $\eta^k = \eta$.

- an alternating method proposed by Friedlander and Weiss [11]. This algorithm is based on a two-step procedure. First, one assumes that the calibration parameters are known, and estimates the frequencies with the MUSIC algorithm. Given the recovered frequencies, one then minimizes the squared sum of the noise-space correlation functions evaluated at the recovered frequencies over all calibration parameters. We pick a random initialization and terminate the iteration while the squared sum of the noise-space correlation functions evaluated at the recovered frequencies only decreases by 10^{-4} or less.

5.1 Partial algebraic method and optimization approach

We expect that the optimization approach outperforms the partial algebraic method in almost all cases since more measurements are used. To illustrate this, we perform reconstructions on 20 frequencies separated by $2/N$. We set $DR_\gamma = DR_g = 2$ and consider a noise level $\sigma = 0.5$. We apply both methods to the same set of measurements. In Fig. 2, the imaging functions in the MUSIC algorithm are displayed for the partial algebraic method and the optimization approach, respectively. Both techniques succeed as imaging functions peak around exact frequencies. In comparison, the optimization approach yields a better result since the peaks are higher and shaper, and the support error is smaller.

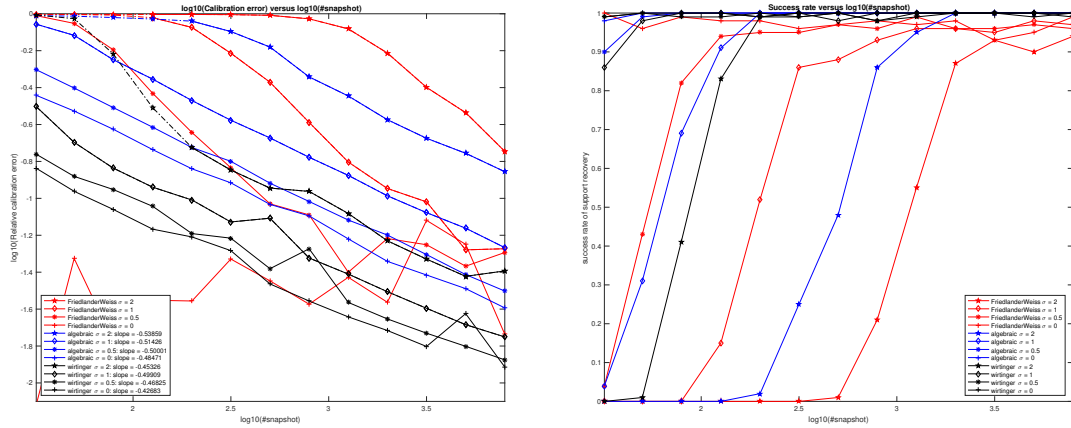


(a) Imaging function in partial algebraic method (b) Imaging function in optimization approach

Figure 2: Imaging functions (after a proper translation) in the MUSIC algorithm for the partial algebraic method (a) and the optimization approach (b) respectively. Red dots represent the locations of true frequencies. The two methods are applied for the same measurements generated by 20 frequencies separated by $2/N$, when $DR_\gamma = DR_g = 2$, $L = 500$ and $\sigma = 0.5$.

5.2 Sensitivity to the number of snapshots

The performance of all algorithms improves as the number of snapshots L increases. We prove in Theorem 2 that, for the partial algebraic method, when the underlying frequencies are separated by $1/N$ or above, the reconstruction error of calibration parameters decays like $O(1/\sqrt{L})$. In order to verify this result, we perform reconstructions on 20 frequencies separated by $2/N$ when L increases from 30 to 10^4 . We set $DR_\gamma = DR_g = 2$, and let the noise level be $\sigma = 0, 0.5, 1, 2$. Fig. 3 displays the relative reconstruction error of calibration parameters and the success probability of support recovery in 100 independent experiments versus L in \log_{10} scale. Frequency support is called successfully recovered if $d(\mathcal{S}, \hat{\mathcal{S}}) \leq 0.2/N$. We observe that, (1) the reconstruction errors of calibration parameters for the partial algebraic method and the optimization approach decay like $O(1/\sqrt{L})$ since the slopes in Fig. 3 (a) are roughly -0.5 ; (2) in terms of stability to the number of snapshots, our optimization approach has the best performance; the partial algebraic method is the second best performer.



(a) Relative calibration error versus L

(b) Frequency support success probability versus L

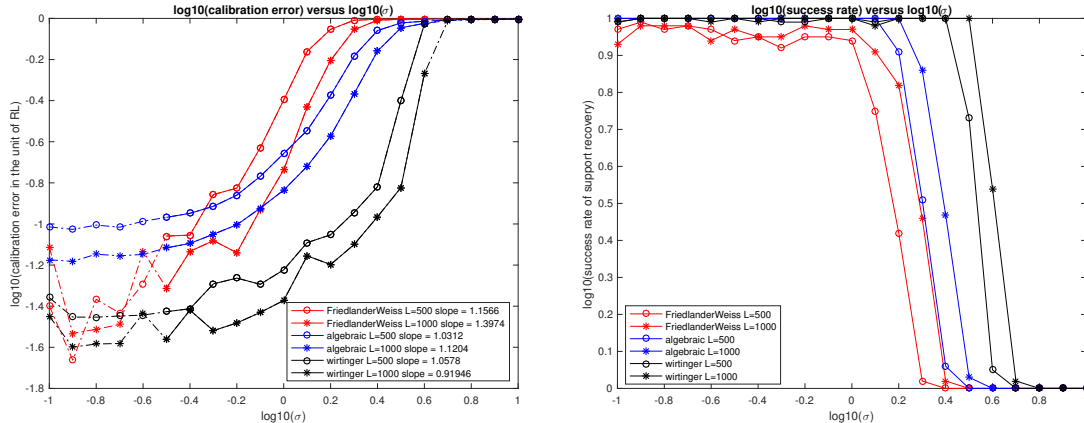
Figure 3: (a) and (b) show the average relative reconstruction error of calibration parameters and the success probability of support recovery in 100 independent experiments versus L in \log_{10} scale. Here 20 frequencies separated by $2/N$, $DR_{\gamma} = DR_g = 2$, and the noise level $\sigma = 0, 0.5, 1, 2$. Frequency support is called successfully recovered if $d(\mathcal{S}, \hat{\mathcal{S}}) \leq 0.2/N$. The slopes are calculated by fitting the solid portion of the curves by a line.

5.3 Sensitivity to noise

To test the sensitivity of various methods to noise, we perform reconstructions on 20 frequencies separated by $2/N$ when σ increases from $10^{-0.5}$ to 10. We set $DR_{\gamma} = DR_g = 2$, and let $L = 500, 1000$ respectively. Frequency support is called successfully recovered if $d(\mathcal{S}, \hat{\mathcal{S}}) \leq 0.2/N$. Figure 4 displays the average reconstruction error of calibration parameters and the success probability of support recovery in 100 independent experiments versus σ in \log_{10} scale. We observe that, (1) the reconstruction errors of calibration parameters for the partial algebraic method and the optimization approach increase like $O(\sigma)$ when $\log_{10} \sigma$ varies from -0.5 to 0.6 since the slopes in Fig. 4 (a) are roughly 1; (2) in terms of stability to noise, our optimization approach has the best performance, while the partial algebraic method is the second best. Notice that the reconstruction errors do not approach 0 when σ decreases to 0 due to deviation of the empirical covariance matrix from the true covariance matrix caused by the finite number of snapshots.

6 Conclusion and future research

This paper studies sensor calibration in spectral estimation with multiple snapshots. We assume the true frequencies are located on a continuous domain and each sensor has an unknown calibration parameter. Uniqueness for the calibration parameters and the frequencies, up to a trivial ambiguity, are proved with infinite snapshots of noiseless measurements, based on the algebraic methods in [19, 31]. Sensitivity analysis of the partial algebraic method [31] with respect to the number of snapshots and noise is presented. While only partial measurements are exploited in the algebraic method, we propose an optimization approach to make full use of the measurements. Superior performance of our optimization approach is demonstrated through a systematic numerical comparison with the partial algebraic method [31] and the alternating



(a) Relative calibration error versus σ in \log_{10} scale (b) Support error versus σ in \log_{10} scale

Figure 4: Reconstruction errors of the calibration parameters and the support versus σ in \log_{10} scale. Here we perform reconstructions on 20 frequencies separated by $2/N$ when σ increases from 0.1 to 10. We set $DR_\gamma = DR_g = 2$, and let $L = 2000, 5000$ respectively. Frequency support is called successfully recovered if $d(\mathcal{S}, \hat{\mathcal{S}}) \leq 0.2/N$. In (a), the slopes are computed by fitting the solid portion of the curves by a line.

method [11].

Several interesting questions are left for future investigations. First, uniqueness in the current paper holds with infinite snapshots of noiseless measurements. It is interesting to study uniqueness with a minimal number of snapshots. Second, we have not proved global convergence of Wirtinger gradient descent in the optimization approach, even though we have observed superior numerical performance with a large class of initializations. In [1, 17, 16], the measurement is bilinear. In our problem, the covariance matrix is quadratic in g and linear in f , which makes the local regularity condition [4, 16] harder to prove. In the future, we will consider the case where the true frequencies are located on the grid with spacing $1/N$, which gives rise to the calibration problem modeled by (5), with the sensing matrix A being a DFT matrix. The DFT matrix is not generic so the uniqueness result in [14] does not apply. When A is a DFT matrix and X has s nonzero rows in (5), it is interesting to study uniqueness with a minimal number of snapshots, and develop algorithms with performance guarantees. We can also formulate an optimization problem and solve it by gradient descent. In this case, the measurement becomes bilinear.

A Sensitivity of the partial algebraic method (Proof of Theorem 2)

A.1 Proof of Theorem 2

The proof of Theorem 2 relies on the following matrix Bernstein inequalities.

Proposition 3 ([28, Theorem 7.3.1]). *Consider a finite sequence $\{X_k\}$ of random Hermitian matrices that satisfy*

$$\mathbb{E}X_k = 0 \quad \text{and} \quad \|X_k\| \leq R.$$

Define the random matrix $Y = \sum_k X_k$. Suppose $\mathbb{E}Y^2 \preceq V$ for some positive semidefinite matrix V and let the intrinsic dimension of V be $\text{intdim}(V) = \text{trace}(V)/\|V\|$. Then for any

$$t \geq \|V\|^{1/2} + R/3,$$

$$\mathbb{P}\{\|Y\| \geq t\} \leq 4 \cdot \text{intdim}(V) \cdot \exp\left(\frac{-t^2/2}{\|V\| + Rt/3}\right)$$

and

$$\mathbb{E}\|Y\| \leq \sqrt{2\|V\| \log(4 \cdot \text{intdim}(V))} + \frac{1}{3}R \log(4 \cdot \text{intdim}(V)).$$

Proof of Theorem 2. In this proof, we assume $\|g\|$ is known, and $\beta_0 = \beta_{N-1} = 0$ to remove trivial ambiguities; otherwise, for g , our estimate gives an upper bound to $\min_{c_0 > 0, c_1, c_2 \in \mathbb{R}} \|c_0 \widehat{g} - e^{ic_1} \text{diag}\{e^{inc_2}\}_{n=0}^{N-1}\} g\|_\infty$.

In the case of finite snapshots, the sampled covariance matrix \widetilde{R}_e^y deviates from R_e^y by:

$$\begin{aligned} \|R_e^y - \widetilde{R}_e^y\| &\leq \|GA(R^x - \widetilde{R}^x)A^*G^* + GA(R^{xe} - \widetilde{R}^{xe}) + (R^{ex} - \widetilde{R}^{ex})A^*G^* + R^e - \widetilde{R}^e\| \\ &\leq \sigma_{\max}^2(G)\sigma_{\max}^2(A)\|R^x - \widetilde{R}^x\| + \sigma_{\max}(G)\sigma_{\max}(A)\|R^{xe} - \widetilde{R}^{xe}\| \\ &\quad + \sigma_{\max}(G)\sigma_{\max}(A)\|R^{ex} - \widetilde{R}^{ex}\| + \|R^e - \widetilde{R}^e\|, \end{aligned}$$

where we use the same notations as (8). We will estimate $\|R^x - \widetilde{R}^x\|$ using the matrix Bernstein inequality in Proposition 3. Let $\widetilde{R}_{x,t} = \frac{1}{L}(x(t)x^*(t) - R^x)$ which satisfies $\|\widetilde{R}_{x,t}\| \leq \frac{1}{L}(\max_{t \in \Gamma} \|x(t)\|^2 + \gamma_{\max}^2)$ for $t \in \Gamma$. Then $\widetilde{R}^x - R^x = \sum_{t \in \Gamma} \widetilde{R}_{x,t}$. We observe that

$$\begin{aligned} \mathbb{E}(\widetilde{R}^x - R^x)^2 &= \sum_{t \in \Gamma} \mathbb{E} \widetilde{R}_{x,t}^2 = \frac{1}{L^2} \sum_{t \in \Gamma} \mathbb{E}(x(t)x^*(t) - R^x)(x(t)x^*(t) - R^x) \\ &\preceq \frac{1}{L} \left(\max_t \|x(t)\|^2 R^x - (R^x)^2 \right) \preceq \frac{\max_t \|x(t)\|^2}{L} R^x, \end{aligned}$$

where R^x has the intrinsic dimension $\text{intdim}(R^x) \leq s$. Applying Proposition 3, we obtain that for any $\eta \geq \frac{\gamma_{\max} \max_t \|x(t)\|}{\sqrt{L}} + \frac{\max_{t \in \Gamma} \|x(t)\|^2 + \gamma_{\max}^2}{3L}$, we have

$$\mathbb{P}\{\|R^x - \widetilde{R}^x\| \geq \eta\} \leq 4s \cdot \exp\left(\frac{-\eta^2/2}{\frac{\gamma_{\max}^2 \max_t \|x(t)\|^2}{L} + \frac{\gamma_{\max}^2 + \max_{t \in \Gamma} \|x(t)\|^2}{3L}}\right), \quad (31)$$

$$\mathbb{E}\|R^x - \widetilde{R}^x\| \leq \frac{\gamma_{\max} \max_t \|x(t)\| \sqrt{2 \log 4s}}{\sqrt{L}} + \frac{\gamma_{\max}^2 + \max_{t \in \Gamma} \|x(t)\|^2}{3L} \log 4s. \quad (32)$$

Similarly, for all $\eta > 0$, we have

$$\mathbb{P}\{\|R^{xe} - \widetilde{R}^{xe}\| \geq \eta\} \leq (N + s) \cdot \exp\left(\frac{-\eta^2/2}{\frac{N\sigma^2\gamma_{\max}^2}{L} + \frac{\max_{t \in \Gamma} \|x(t)\| \|e(t)\|}{3L}}\right), \quad (33)$$

$$\mathbb{P}\{\|R^e - \widetilde{R}^e\| \geq \eta\} \leq 2N \cdot \exp\left(\frac{-\eta^2/2}{\frac{\sigma^2 \max_t \|e(t)\|^2}{L} + \frac{\sigma^2 + \max_{t \in \Gamma} \|e(t)\|^2}{3L}}\right), \quad (34)$$

and

$$\mathbb{E}\|R^{xe} - \widetilde{R}^{xe}\| \lesssim \frac{\sigma \gamma_{\max} \sqrt{2N \log(N + s)}}{\sqrt{L}} + \frac{\max_{t \in \Gamma} \|x(t)\| \|e(t)\|}{3L} \log(N + s), \quad (35)$$

$$\mathbb{E}\|R^e - \widetilde{R}^e\| \lesssim \frac{\sigma \max_t \|e(t)\| \sqrt{2 \log 2N}}{\sqrt{L}} + \frac{\sigma^2 + \max_{t \in \Gamma} \|e(t)\|^2}{3L} \log 2N, \quad (36)$$

where we apply the matrix Bernstein inequality for non-Hermitian case [28, Theorem 1.6.2] to estimate $\|R^{xe} - \tilde{R}^{xe}\|$. Our estimator of R^y is $\hat{R}^y = \tilde{R}_e^y - \hat{\sigma}^2 I_N$, which has the following error

$$\|R^y - \hat{R}^y\| = \|(R_e^y - \sigma^2 I_N) - (\tilde{R}_e^y - \hat{\sigma}^2 I_N)\| \leq \|R_e^y - \tilde{R}_e^y\| + |\sigma^2 - \hat{\sigma}^2| \leq 2\|R_e^y - \tilde{R}_e^y\|, \quad (37)$$

where the last inequality follows from the Weyl's inequality [30]. Combining (32), (35), (36) and (37) gives rise to $\mathbb{E}\|R^y - \hat{R}^y\| \leq \Delta R^y$ with ΔR^y defined in (19).

Define the event

$$\mathcal{E} := \left\{ \max(\alpha_{\max}^2 \sigma_{\max}^2(A) \|R^x - \tilde{R}^x\|, \alpha_{\max} \sigma_{\max}(A) \|R^{xe} - \tilde{R}^{xe}\|, \|R^e - \tilde{R}^e\|) \leq \frac{\alpha_{\min}^2 |f_1|}{16} \right\}$$

under which we have

$$\|R^y - \hat{R}^y\| \leq \frac{1}{2} \alpha_{\min}^2 |f_1| \leq \frac{1}{2} \alpha_{\min}^2 f_0.$$

This implies that

$$\text{trace}(\hat{R}^y) \geq \text{trace} R^y - N \|R^y - \hat{R}^y\| = \|g\|^2 f_0 - \frac{1}{2} N \alpha_{\min}^2 f_0 \geq \frac{1}{2} \|g\|^2 f_0 = \frac{1}{2} \text{trace}(R^y),$$

and $\text{trace}(\hat{R}^y) \leq 3/2 \text{trace}(R^y)$. We first perform all estimates under the event \mathcal{E} and consider \mathcal{E}^c later.

Condition on \mathcal{E}

In the partial algebraic method, if $\|g\|$ is known, then α can be recovered without any scaling ambiguity. The exact and recovered calibration phases are:

$$\alpha_n^2 = \frac{R_{n,n}^y}{\text{trace}(R^y)} \|g\|^2 \quad \hat{\alpha}_n^2 = \frac{\hat{R}_{n,n}^y}{\text{trace}(\hat{R}^y)} \|g\|^2. \quad (38)$$

Hence

$$\begin{aligned} |\alpha_n^2 - \hat{\alpha}_n^2| &\leq \left| \frac{R_{n,n}^y}{\text{trace}(R^y)} - \frac{\hat{R}_{n,n}^y}{\text{trace}(\hat{R}^y)} \right| \|g\|^2 = \left| \frac{R_{n,n}^y \text{trace}(\hat{R}^y) - \hat{R}_{n,n}^y \text{trace}(R^y)}{\text{trace}(R^y) \text{trace}(\hat{R}^y)} \right| \|g\|^2 \\ &\leq \frac{R_{n,n}^y |\text{trace}(\hat{R}^y) - \text{trace}(R^y)| + \text{trace}(R^y) |\hat{R}_{n,n}^y - R_{n,n}^y|}{\text{trace}(R^y) \text{trace}(\hat{R}^y)} \|g\|^2 \\ &\leq \frac{|g_n|^2 f_0 N + \|g\|^2 f_0}{\|g\|^2 f_0 \|g\|^2 f_0 / 2} \|g\|^2 \|R^y - \hat{R}^y\| = 2 \frac{N |g_n|^2 + \|g\|^2}{\|g\|^2 f_0} \|R^y - \hat{R}^y\|. \end{aligned}$$

On the other hand,

$$\alpha_n^2 = \frac{|g_n|^2 f_0}{\text{trace} R^y} \|g\|^2 \quad \hat{\alpha}_n^2 \geq \frac{R_{n,n}^y - \|R^y - \hat{R}^y\|}{\frac{3}{2} \text{trace} R^y} \|g\|^2 \geq \frac{|g_n|^2 f_0 - \frac{1}{2} |g_n|^2 f_0}{\frac{3}{2} \text{trace} R^y} \|g\|^2 \geq \frac{\alpha_n^2}{3},$$

in the event \mathcal{E} and then

$$\begin{aligned} |\alpha_n - \hat{\alpha}_n| &= \frac{|\alpha_n^2 - \hat{\alpha}_n^2|}{\alpha_n + \hat{\alpha}_n} \leq \frac{1}{4\alpha_n/3} \cdot 2 \frac{\|g\|^2 + N |g_n|^2}{\|g\|^2 f_0} \cdot \|R^y - \hat{R}^y\|, \\ \|\alpha - \hat{\alpha}\|_\infty &\leq \frac{3}{2\alpha_{\min}} \cdot \frac{\|g\|^2 + N \alpha_{\max}^2}{\|g\|^2 f_0} \cdot \|R^y - \hat{R}^y\|. \end{aligned}$$

Next we estimate $\|\beta - \widehat{\beta}\|_\infty$. To remove trivial ambiguities, we assume the exact calibration phases β satisfy

$$\Phi\beta = b \quad \text{where } b_0 = b_{N-1} = 0, \quad b_n = \angle \frac{R_{n+1,n}^y}{R_{n,n-1}^y}, \quad n = 1, \dots, N-2.$$

Our recovered calibration phases $\widehat{\beta}$ are:

$$\Phi\widehat{\beta} = \widehat{b} \quad \text{where } \widehat{b}_0 = \widehat{b}_{N-1} = 0, \quad \widehat{b}_n = \angle \frac{\widehat{R}_{n+1,n}^y}{\widehat{R}_{n,n-1}^y}, \quad n = 1, \dots, N-2.$$

Recall that $R_{n,n-1}^y = \alpha_n \alpha_{n-1} e^{i(\beta_n - \beta_{n-1})} f_1$, so $\alpha_{\min}^2 |f_1| \leq |R_{n,n-1}^y| \leq \alpha_{\max}^2 |f_1|$. In the event \mathcal{E} , $\alpha_{\min}^2 |f_1|/2 \leq |\widehat{R}_{n,n-1}^y| \leq 3\alpha_{\max}^2 |f_1|/2$, and

$$\left| \frac{R_{n+1,n}^y}{R_{n,n-1}^y} - \frac{\widehat{R}_{n+1,n}^y}{\widehat{R}_{n,n-1}^y} \right| = \frac{|R_{n+1,n}^y \widehat{R}_{n,n-1}^y - R_{n,n-1}^y \widehat{R}_{n+1,n}^y|}{|R_{n,n-1}^y \widehat{R}_{n,n-1}^y|} \leq 4 \frac{\alpha_{\max}^2}{\alpha_{\min}^4 |f_1|^2} \|R^y - \widehat{R}^y\|.$$

For any $z, \widehat{z} \in \mathbb{C}$, $|(\angle z - \angle \widehat{z}) \bmod 2\pi| \leq \frac{4|z - \widehat{z}|}{\min(|z|, |\widehat{z}|)}$ whenever $|z - \widehat{z}| \leq \min(|z|, |\widehat{z}|)$. Hence

$$\begin{aligned} \|b - \widehat{b}\|_\infty &= \max_n \left| \left(\angle \frac{R_{n+1,n}^y}{R_{n,n-1}^y} - \angle \frac{\widehat{R}_{n+1,n}^y}{\widehat{R}_{n,n-1}^y} \right) \bmod 2\pi \right| \\ &\leq \max_n \frac{4 \left| \frac{R_{n+1,n}^y}{R_{n,n-1}^y} - \frac{\widehat{R}_{n+1,n}^y}{\widehat{R}_{n,n-1}^y} \right|}{\min \left(\left| \frac{R_{n+1,n}^y}{R_{n,n-1}^y} \right|, \left| \frac{\widehat{R}_{n+1,n}^y}{\widehat{R}_{n,n-1}^y} \right| \right)} \leq \frac{48\alpha_{\max}^4}{\alpha_{\min}^4} \cdot \frac{\|R^y - \widehat{R}^y\|}{\alpha_{\min}^2 |f_1|^2} \end{aligned}$$

whenever $\|R^y - \widehat{R}^y\| \leq \frac{\alpha_{\min}^6 |f_1|^2}{12\alpha_{\max}^4}$; for simplicity, we assume that $|f_1| \geq \frac{6\alpha_{\max}^2}{\alpha_{\min}^2}$ so that $\|R^y - \widehat{R}^y\|$ satisfies this constraint in the event \mathcal{E} . The infinity norm of the matrix Φ^{-1} is upper bounded by (see [12, Chapter 2]):

$$\|\Phi^{-1}\|_\infty = \max_j \sum_{i=0}^{N-1} |\Phi_{i,j}^{-1}| \leq 3N^2.$$

Therefore

$$\|\beta - \widehat{\beta}\|_\infty \leq \|\Phi^{-1}\|_\infty \|b - \widehat{b}\|_\infty \leq 144N^2 \frac{\alpha_{\max}^4}{\alpha_{\min}^4} \cdot \frac{\|R^y - \widehat{R}^y\|}{\alpha_{\min}^2 |f_1|^2}.$$

Combining the estimates of $\|\alpha - \widehat{\alpha}\|_\infty$ and $\|\beta - \widehat{\beta}\|_\infty$ gives rise to

$$\|g - \widehat{g}\|_\infty = \max_n |g_n - \widehat{g}_n| \leq \max_n |\alpha_n| |e^{i\beta_n} - e^{i\widehat{\beta}_n}| + |\alpha_n - \widehat{\alpha}_n| \leq \|\alpha - \widehat{\alpha}\|_\infty + \alpha_{\max} \|\beta - \widehat{\beta}\|_\infty.$$

As for the input matrix for the MUSIC algorithm, we have

$$F = \text{diag}(g)^{-1} R^y \text{diag}(\widehat{g})^{-1} \quad \widehat{F} = \text{diag}(\widehat{g})^{-1} \widehat{R}^y \text{diag}(\widehat{g})^{-1}.$$

Then

$$\begin{aligned} \|F - \widehat{F}\| &\leq \frac{1}{\widehat{\alpha}_{\min}^2} \|R^y - \widehat{R}^y\| + \frac{\|R^y\|}{\alpha_{\min}} \max_n \left| \frac{1}{g_n} - \frac{1}{\widehat{g}_n} \right| + \frac{\|R^y\|}{\widehat{\alpha}_{\min}} \max_n \left| \frac{1}{g_n} - \frac{1}{\widehat{g}_n} \right| \\ &\leq 9 \frac{\|R^y - \widehat{R}^y\|}{\alpha_{\min}^2} + 12 \frac{\|R^y\|}{\alpha_{\min}^3} \|g - \widehat{g}\|_\infty \leq 9 \frac{\|R^y - \widehat{R}^y\|}{\alpha_{\min}^2} + 12 \frac{\alpha_{\max}^2 \gamma_{\max}^2 \sigma_{\max}^2(A)}{\alpha_{\min}^3} \|g - \widehat{g}\|_\infty. \end{aligned}$$

When the input of MUSIC is \widehat{F} , Proposition 2 gives an estimate on the perturbation of the noise-space correlation function:

$$|\widehat{\mathcal{R}}(\omega) - \mathcal{R}(\omega)| \leq \frac{4\gamma_{\max}^2 \sigma_{\max}^2(A) + 2\|F - \widehat{F}\|}{(\gamma_{\min}^2 \sigma_{\min}^2(A) - \|F - \widehat{F}\|)^2} \cdot \|F - \widehat{F}\|.$$

Conditioning on the event \mathcal{E} , we have

$$\begin{aligned} \mathbb{E}(\|g - \widehat{g}\|_{\infty} | \mathcal{E}) &\leq \mathbb{E}(\|\alpha - \widehat{\alpha}\|_{\infty} | \mathcal{E}) + \alpha_{\max} \mathbb{E}(\|\beta - \widehat{\beta}\|_{\infty} | \mathcal{E}) \\ &\leq \frac{3(\|g\|^2 + N\alpha_{\max}^2)}{2\alpha_{\min}\|g\|^2 f_0} \Delta R^y + 144N^2 \frac{\alpha_{\max}^5}{\alpha_{\min}^6 |f_1|^2} \Delta R^y \end{aligned}$$

and

$$\mathbb{E}(\|F - \widehat{F}\| | \mathcal{E}) \leq 9 \frac{\Delta R^y}{\alpha_{\min}^2} + \frac{12\alpha_{\max}^2 \gamma_{\max}^2 \sigma_{\max}^2(A)}{\alpha_{\min}^3} \left(\frac{3(\|g\|^2 + N\alpha_{\max}^2)}{2\alpha_{\min}\|g\|^2 f_0} + 144N^2 \frac{\alpha_{\max}^5}{\alpha_{\min}^6 |f_1|^2} \right) \Delta R^y.$$

Condition on \mathcal{E}^c

Finally we consider the event \mathcal{E}^c which occurs with small probability when L is sufficiently large:

$$\begin{aligned} \mathbb{P}\{\mathcal{E}^c\} &\leq \mathbb{P}\left\{ \|R^x - \widetilde{R}^x\| \geq \frac{\alpha_{\min}^2 |f_1|}{16\alpha_{\max}^2 \sigma_{\max}^2(A)} \right\} + \mathbb{P}\left\{ \|R^{xe} - \widetilde{R}^{xe}\| \geq \frac{\alpha_{\min}^2 |f_1|}{16\alpha_{\max} \sigma_{\max}(A)} \right\} \\ &\quad + \mathbb{P}\left\{ \|R^e - \widetilde{R}^e\| \geq \frac{\alpha_{\min}^2 |f_1|}{16} \right\} \\ &\leq 4N e^{-LC(\alpha_{\max}, \alpha_{\min}, \gamma_{\max}, \sigma_{\max}(A), |f_1|, \sigma, \max_t \|x(t)\|, \max_t \|e(t)\|)} \end{aligned}$$

for some positive constant $C(\alpha_{\max}, \alpha_{\min}, \gamma_{\max}, \sigma_{\max}(A), |f_1|, \sigma, \max_t \|x(t)\|, \max_t \|e(t)\|)$. In any case, $\|g - \widehat{g}\|_{\infty} \leq \|g\|_{\infty} + \|\widehat{g}\|_{\infty} \leq \|g\|_{\infty} + \|g\| \leq 2\|g\|$, where $\|\widehat{g}\|_{\infty} \leq \|g\|$ due to (38). Therefore,

$$\begin{aligned} \mathbb{E}\|g - \widehat{g}\|_{\infty} &\leq \mathbb{E}(\|g - \widehat{g}\|_{\infty} | \mathcal{E}) \mathbb{P}\{\mathcal{E}\} + 2\|g\| \mathbb{P}\{\mathcal{E}^c\} \\ &\leq \frac{3(\|g\|^2 + N\alpha_{\max}^2)}{2\alpha_{\min}\|g\|^2 f_0} \Delta R^y + 144N^2 \frac{\alpha_{\max}^5}{\alpha_{\min}^6 |f_1|^2} \Delta R^y + 8N\|g\|_2 e^{-LC}. \end{aligned} \quad (39)$$

Since the the first two terms in (39) is $O(1/L)$ and the last term is $O(e^{-CL})$, we can guarantee (20) when L is sufficiently large. A similar estimate holds for $\|F - \widehat{F}\|$. \square

B Proof of Lemma 2

According to (12), we have

$$|g_n|^2 = \frac{R_{n,n}^y}{f_0}, \quad n = 0, \dots, N-1,$$

and for any $k = 1, \dots, N-1$

$$|f_k|^2 = \frac{|R_{n+k,n}^y|^2}{|g_{n+k}|^2 |g_n|^2} = \frac{f_0^2 |R_{n+k,n}^y|^2}{R_{n+k,n+k}^y R_{n,n}^y} \quad \text{for any } 0 \leq n \leq N-k-1.$$

Therefore

$$\|g\|^2 = \frac{\sum_{n=0}^{N-1} R_{n,n}^y}{f_0}$$

and

$$\begin{aligned}\|f\| &= \sqrt{\sum_{k=0}^{N-1} |f_k|^2} = \sqrt{f_0^2 + \sum_{k=1}^{N-1} \frac{1}{N-k} \sum_{n=0}^{N-k-1} \frac{f_0^2 |R_{n+k,n}^y|^2}{R_{n+k,n+k}^y R_{n,n}^y}} \\ &= f_0 \sqrt{1 + \frac{1}{N-k} \sum_{k=1}^{N-1} \sum_{n=0}^{N-k-1} \frac{|R_{n+k,n}^y|^2}{R_{n+k,n+k}^y R_{n,n}^y}}\end{aligned}$$

which gives rise to Lemma 2.

C Proof of Theorem 3

We first show that $\nabla \tilde{\mathcal{L}}$, restricted within $\mathcal{N}_{\hat{n}_0}$, is a Lipschitz function. Notice that g are the exact calibration parameters and f is defined in (6).

Lemma 3. *For any $z := (\mathbf{g}; \mathbf{f})$ and $\Delta \mathbf{z} := (\Delta \mathbf{g}; \Delta \mathbf{f})$ such that $\mathbf{z}, \mathbf{z} + \Delta \mathbf{z} \in \mathcal{N}_{\hat{n}_0}$, $\nabla \tilde{\mathcal{L}}$ is Lipschitz such that*

$$\|\nabla \tilde{\mathcal{L}}(\mathbf{z} + \Delta \mathbf{z}) - \nabla \tilde{\mathcal{L}}(\mathbf{z})\| \leq C_{\text{Lip}} \|\Delta \mathbf{z}\|$$

with

$$C_{\text{Lip}} \leq 146 \hat{n}_0 \max(\sqrt{\hat{n}_0}, \sqrt[4]{\hat{n}_0}) + 8 \hat{n}_0 + 16 \max(\sqrt{\hat{n}_0}, \sqrt[4]{\hat{n}_0}) \|R^y - \hat{R}^y\|_F + \frac{8\rho}{\min(\hat{n}_0, \sqrt{\hat{n}_0})}$$

where $\rho \geq \frac{3\hat{n}_0 + \|R^y - \hat{R}^y\|_F}{(\sqrt{2}-1)^2}$.

Proof of Lemma 3. The Wirtinger gradient of $\tilde{\mathcal{L}}$ is

$$\nabla \tilde{\mathcal{L}} = (\nabla_{\mathbf{g}} \tilde{\mathcal{L}}; \nabla_{\mathbf{f}} \tilde{\mathcal{L}}) = (\nabla_{\mathbf{g}} \mathcal{L} + \nabla_{\mathbf{g}} \mathcal{G}; \nabla_{\mathbf{f}} \mathcal{L} + \nabla_{\mathbf{f}} \mathcal{G}). \quad (40)$$

Part 1: We estimate the upper bound of $\|\nabla_{\mathbf{g}} \mathcal{L}(\mathbf{z} + \mathbf{w}) - \nabla_{\mathbf{g}} \mathcal{L}(\mathbf{z})\|$. Recall that $R^y = \mathbb{E}y(t)y(t)^*$, and

$$\nabla_{\mathbf{g}} \mathcal{L}(z) = 2 \text{diag} \left[\overline{\mathcal{H}(\mathbf{f})^* \text{diag}(\bar{\mathbf{g}}) \left(\text{diag}(\mathbf{g}) \mathcal{H}(\mathbf{f}) \text{diag}(\bar{\mathbf{g}}) - \text{diag}(g) \mathcal{H}(f) \text{diag}(\bar{g}) + R^y - \hat{R}^y \right)} \right].$$

Notice that for any $\mathbf{f}, \mathbf{g}, \mathbf{g}_1, \mathbf{g}_2, \mathbf{h} \in \mathbb{C}^N$ and $X \in \mathbb{C}^{N \times N}$, we have

$$\begin{aligned}\|\text{diag}[\mathcal{H}(\mathbf{f})^* \text{diag}(\mathbf{g}_1) \mathcal{H}(\mathbf{h}) \text{diag}(\mathbf{g}_2)]\| &\leq \|\mathbf{f}\| \|\mathbf{g}_1\| \|\mathbf{h}\| \|\mathbf{g}_2\| \\ \|\text{diag}[\mathcal{H}(\mathbf{f})^* \text{diag}(\mathbf{g}) X]\| &\leq \sqrt{2} \|\mathbf{f}\| \|\mathbf{g}\| \|X\|_F.\end{aligned}$$

For any $\mathbf{z}, \mathbf{z} + \Delta\mathbf{z} \in \mathcal{N}_{\hat{n}_0}$, we have

$$\begin{aligned}
& \|\nabla_{\mathbf{g}}\mathcal{L}(\mathbf{z} + \Delta\mathbf{z}) - \nabla_{\mathbf{g}}\mathcal{L}(\mathbf{z})\| \\
& \leq 2 \left\| \text{diag} \left[\mathcal{H}(\mathbf{f} + \Delta\mathbf{f})^* \text{diag}(\bar{\mathbf{g}} + \overline{\Delta\mathbf{g}}) \text{diag}(\mathbf{g} + \Delta\mathbf{g}) \mathcal{H}(\mathbf{f} + \Delta\mathbf{f}) \text{diag}(\bar{\mathbf{g}} + \overline{\Delta\mathbf{g}}) \right. \right. \\
& \quad \left. \left. - \mathcal{H}(\mathbf{f})^* \text{diag}(\bar{\mathbf{g}}) \text{diag}(\mathbf{g}) \mathcal{H}(\mathbf{f}) \text{diag}(\bar{\mathbf{g}}) \right] \right\| \\
& \quad + 2 \left\| \text{diag} \left[\mathcal{H}(\mathbf{f} + \Delta\mathbf{f})^* \text{diag}(\bar{\mathbf{g}} + \overline{\Delta\mathbf{g}}) \text{diag}(g) \mathcal{H}(f) \text{diag}(\bar{g}) - \mathcal{H}(\mathbf{f})^* \text{diag}(\bar{\mathbf{g}}) \text{diag}(g) \mathcal{H}(f) \text{diag}(\bar{g}) \right] \right\| \\
& \quad + 2 \left\| \text{diag} \left[\mathcal{H}(\mathbf{f} + \Delta\mathbf{f})^* \text{diag}(\bar{\mathbf{g}} + \overline{\Delta\mathbf{g}}) (R^y - \hat{R}^y) - \mathcal{H}(\mathbf{f})^* \text{diag}(\bar{\mathbf{g}}) (R^y - \hat{R}^y) \right] \right\| \\
& \leq 2 \left(\|\Delta\mathbf{f}\| \|\mathbf{g} + \Delta\mathbf{g}\|^3 \|\mathbf{f} + \Delta\mathbf{f}\| + \|\mathbf{f}\| \|\Delta\mathbf{g}\| \|\mathbf{g} + \Delta\mathbf{g}\|^2 \|\mathbf{f} + \Delta\mathbf{f}\| + \|\mathbf{f}\| \|\mathbf{g}\| \|\Delta\mathbf{g}\| \|\mathbf{g} + \Delta\mathbf{g}\| \|\mathbf{f} + \Delta\mathbf{f}\| \right. \\
& \quad \left. + \|\mathbf{f}\| \|\mathbf{g}\|^2 \|\Delta\mathbf{f}\| \|\mathbf{g} + \Delta\mathbf{g}\| + \|\mathbf{f}\|^2 \|\mathbf{g}\|^2 \|\Delta\mathbf{g}\| + \|\Delta\mathbf{f}\| \|\mathbf{g} + \Delta\mathbf{g}\| \|g\|^2 \|f\| + \|\mathbf{f}\| \|\Delta\mathbf{g}\| \|g\|^2 \|f\| \right) \\
& \quad + 2\sqrt{2} \left(\|\Delta\mathbf{f}\| \|\mathbf{g} + \Delta\mathbf{g}\| \|R^y - \hat{R}^y\|_F + \|\mathbf{f}\| \|\Delta\mathbf{g}\| \|R^y - \hat{R}^y\|_F \right) \\
& \leq 64\hat{n}_0\sqrt{\hat{n}_0} \|\Delta\mathbf{g}\| + 24\sqrt{2}\hat{n}_0\hat{n}_0^{\frac{1}{4}} \|\Delta\mathbf{f}\| + 4\hat{n}_0^{\frac{1}{4}} \|R^y - \hat{R}^y\|_F \|\Delta\mathbf{f}\| + 4\sqrt{2}\hat{n}_0 \|\Delta\mathbf{g}\| \|R^y - \hat{R}^y\|_F. \tag{41}
\end{aligned}$$

Part 2: We estimate the upper bound of $\|\nabla_{\mathbf{f}}\mathcal{L}(\mathbf{z} + \Delta\mathbf{z}) - \nabla_{\mathbf{f}}\mathcal{L}(\mathbf{z})\|$. Notice that for any $\mathbf{g}_1, \mathbf{g}_2, \mathbf{f} \in \mathbb{C}^N$ and $X \in \mathbb{C}^{N \times N}$, we have

$$\begin{aligned}
\|\mathcal{H}^a[\text{diag}(\mathbf{g}_1)\mathcal{H}(\mathbf{f})\text{diag}(\mathbf{g}_2)]\| & \leq 2\|\mathbf{g}_1\| \|\mathbf{f}\| \|\mathbf{g}_2\|, \\
\|\mathcal{H}^a[\text{diag}(\mathbf{g}_1)X\text{diag}(\mathbf{g}_2)]\| & \leq 2\|\mathbf{g}_1\| \|\mathbf{g}_2\| \|X\|_F.
\end{aligned}$$

By using triangle inequalities, we obtain

$$\begin{aligned}
& \|\nabla_{\mathbf{f}}\mathcal{L}(\mathbf{z} + \Delta\mathbf{z}) - \nabla_{\mathbf{f}}\mathcal{L}(\mathbf{z})\| \\
& \leq \left\| \mathcal{H}^a \left[\text{diag}(\overline{\mathbf{g} + \Delta\mathbf{g}}) \text{diag}(\mathbf{g} + \Delta\mathbf{g}) \mathcal{H}(\mathbf{f} + \Delta\mathbf{f}) \text{diag}(\overline{\mathbf{g} + \Delta\mathbf{g}}) \text{diag}(\mathbf{g} + \Delta\mathbf{g}) \right. \right. \\
& \quad \left. \left. - \text{diag}(\bar{\mathbf{g}}) \text{diag}(\mathbf{g}) \mathcal{H}(\mathbf{f}) \text{diag}(\bar{\mathbf{g}}) \text{diag}(\mathbf{g}) \right] \right\| \\
& \quad + \left\| \mathcal{H}^a \left[\text{diag}(\overline{\mathbf{g} + \Delta\mathbf{g}}) \text{diag}(g) \mathcal{H}(f) \text{diag}(\bar{g}) \text{diag}(\mathbf{g} + \Delta\mathbf{g}) - \text{diag}(\bar{\mathbf{g}}) \text{diag}(g) \mathcal{H}(f) \text{diag}(\bar{g}) \text{diag}(\mathbf{g}) \right] \right\| \\
& \quad + \left\| \mathcal{H}^a \left[\text{diag}(\overline{\mathbf{g} + \Delta\mathbf{g}}) (R^y - \hat{R}^y) \text{diag}(\mathbf{g} + \Delta\mathbf{g}) - \text{diag}(\bar{\mathbf{g}}) (R^y - \hat{R}^y) \text{diag}(\mathbf{g}) \right] \right\| \\
& \leq 2 \left\| |\mathbf{g} + \Delta\mathbf{g}|^2 - |\mathbf{g}|^2 \right\| \cdot \|\mathbf{f} + \Delta\mathbf{f}\| \cdot \left\| |\mathbf{g} + \Delta\mathbf{g}|^2 \right\| + 2 \left\| |\mathbf{g}|^2 \right\| \cdot \|\Delta\mathbf{f}\| \cdot \left\| |\mathbf{g} + \Delta\mathbf{g}|^2 \right\| \\
& \quad + 2 \left\| |\mathbf{g}|^2 \right\| \cdot \|\mathbf{f}\| \cdot \left\| |\mathbf{g} + \Delta\mathbf{g}|^2 - |\mathbf{g}|^2 \right\| + 2\|\Delta\mathbf{g}\| \cdot \|g\|^2 \cdot \|f\| \cdot \|\mathbf{g} + \Delta\mathbf{g}\| + 2\|\mathbf{g}\| \cdot \|g\|^2 \cdot \|f\| \cdot \|\Delta\mathbf{g}\| \\
& \quad + 2\|\Delta\mathbf{g}\| \cdot \|R^y - \hat{R}^y\|_F \cdot \|\mathbf{g} + \Delta\mathbf{g}\| + 2\|\mathbf{g}\| \cdot \|R^y - \hat{R}^y\|_F \cdot \|\Delta\mathbf{g}\|.
\end{aligned}$$

Whenever $\mathbf{z}, \mathbf{z} + \Delta\mathbf{z} \in \mathcal{N}_{\hat{n}_0}$, we have

$$\|\Delta\mathbf{g}\| \leq 2\sqrt{2}\hat{n}_0^{\frac{1}{4}}, \quad \left\| |\mathbf{g} + \Delta\mathbf{g}|^2 - |\mathbf{g}|^2 \right\| \leq 2\sqrt{2}\hat{n}_0^{\frac{1}{4}} \|\Delta\mathbf{g}\|$$

and therefore

$$\|\nabla_{\mathbf{f}}\mathcal{L}(\mathbf{z} + \Delta\mathbf{z}) - \nabla_{\mathbf{f}}\mathcal{L}(\mathbf{z})\| \leq 48\sqrt{2}\hat{n}_0\hat{n}_0^{\frac{1}{4}} \|\Delta\mathbf{g}\| + 8\hat{n}_0 \|\Delta\mathbf{f}\| + 4\sqrt{2}\hat{n}_0^{\frac{1}{4}} \|R^y - \hat{R}^y\|_F \|\Delta\mathbf{g}\|. \tag{42}$$

Part 3: We estimate the upper bound of $\|\nabla_{\mathbf{f}}\mathcal{G}(\mathbf{z} + \Delta\mathbf{z}) - \nabla_{\mathbf{f}}\mathcal{G}(\mathbf{z})\|$ and $\|\nabla_{\mathbf{g}}\mathcal{G}(\mathbf{z} + \Delta\mathbf{z}) - \nabla_{\mathbf{g}}\mathcal{G}(\mathbf{z})\|$. Notice that $\mathcal{G}'_0(z) = 2 \max(z - 1, 0)$ and hence

$$|\mathcal{G}'_0(z_1) - \mathcal{G}'_0(z_2)| \leq 2|z_1 - z_2|, \quad \mathcal{G}'_0(z) \leq 2|z|, \quad \forall z_1, z_2, z \in \mathbb{R}.$$

For any $\mathbf{z}, \mathbf{z} + \Delta\mathbf{z} \in \mathcal{N}_{\hat{n}_0}$, we have

$$\begin{aligned}
\|\nabla_{\mathbf{f}}\mathcal{G}(\mathbf{z} + \Delta\mathbf{z}) - \nabla_{\mathbf{f}}\mathcal{G}(\mathbf{z})\| &= \frac{\rho}{2\hat{n}_0} \left\| \mathcal{G}'_0 \left(\frac{\|\mathbf{f} + \Delta\mathbf{f}\|^2}{2\hat{n}_0} \right) (\mathbf{f} + \Delta\mathbf{f}) - \mathcal{G}'_0 \left(\frac{\|\mathbf{f}\|^2}{2\hat{n}_0} \right) \mathbf{f} \right\| \\
&\leq \frac{\rho}{2\hat{n}_0} \left| \mathcal{G}'_0 \left(\frac{\|\mathbf{f} + \Delta\mathbf{f}\|^2}{2\hat{n}_0} \right) - \mathcal{G}'_0 \left(\frac{\|\mathbf{f}\|^2}{2\hat{n}_0} \right) \right| \|\mathbf{f} + \Delta\mathbf{f}\| + \frac{\rho}{2\hat{n}_0} \mathcal{G}'_0 \left(\frac{\|\mathbf{f}\|^2}{2\hat{n}_0} \right) \|\Delta\mathbf{f}\| \\
&\leq \frac{\rho}{2\hat{n}_0} \frac{2(\|\mathbf{f} + \Delta\mathbf{f}\| + \|\mathbf{f}\|)(\|\mathbf{f} + \Delta\mathbf{f}\| - \|\mathbf{f}\|)}{2\hat{n}_0} \|\mathbf{f} + \Delta\mathbf{f}\| + \frac{\rho}{2\hat{n}_0} \cdot \frac{2\|\mathbf{f}\|^2}{2\hat{n}_0} \|\Delta\mathbf{f}\| \leq \frac{6\rho}{\hat{n}_0} \|\Delta\mathbf{f}\|.
\end{aligned} \tag{43}$$

and

$$\|\nabla_{\mathbf{g}}\mathcal{G}(\mathbf{z} + \Delta\mathbf{z}) - \nabla_{\mathbf{g}}\mathcal{G}(\mathbf{z})\| \leq \frac{6\rho}{\sqrt{\hat{n}_0}} \|\Delta\mathbf{g}\|. \tag{44}$$

Combining (40), (41), (42), (43), (44) gives rise to

$$\begin{aligned}
&\|\nabla\tilde{\mathcal{L}}(\mathbf{z} + \Delta\mathbf{z}) - \nabla\tilde{\mathcal{L}}(\mathbf{z})\| \\
&\leq \left(64\hat{n}_0\sqrt{\hat{n}_0} + 48\sqrt{2}\hat{n}_0^4\sqrt{\hat{n}_0} + 4\sqrt{2\hat{n}_0}\|R^y - \hat{R}^y\|_F + 4\sqrt{2}\sqrt[4]{\hat{n}_0}\|R^y - \hat{R}^y\|_F + \frac{6\rho}{\sqrt{\hat{n}_0}} \right) \|\Delta\mathbf{g}\| \\
&\quad + \left(24\sqrt{2}\hat{n}_0^4\sqrt{\hat{n}_0} + 8\hat{n}_0 + 4\sqrt[4]{\hat{n}_0}\|R^y - \hat{R}^y\|_F + \frac{6\rho}{\hat{n}_0} \right) \|\Delta\mathbf{f}\| \\
&\leq \left(166\hat{n}_0 \max(\sqrt{\hat{n}_0}, \sqrt[4]{\hat{n}_0}) + 8\hat{n}_0 + 16 \max(\sqrt{\hat{n}_0}, \sqrt[4]{\hat{n}_0})\|R^y - \hat{R}^y\|_F + \frac{12\rho}{\min(\hat{n}_0, \sqrt{\hat{n}_0})} \right) \|\Delta\mathbf{z}\|.
\end{aligned}$$

□

The proof of Theorem 3 is given below.

Proof of Theorem 3. This proof consists of two parts. In Part 1, we will prove that $(\mathbf{g}^k, \mathbf{f}^k) \in \mathcal{N}_{\hat{n}_0}$ for every k , so $\nabla\tilde{\mathcal{L}}$ always satisfies the Lipschitz property in Lemma 3. In Part 2, we will prove the convergence of the gradient descent algorithm.

Part 1: In the optimization approach, we assume $\hat{n}_0 = \|g\|^2\|f\|$ is known, and start with an initial point $(\mathbf{g}^0, \mathbf{f}^0)$ satisfying $\|\mathbf{g}^0\| \leq \sqrt[4]{2\hat{n}_0}$, $\|\mathbf{f}^0\| \leq \sqrt{2\hat{n}_0}$. Notice that for any $\mathbf{g}, \mathbf{f}, \mathbf{h} \in \mathbb{C}^N$, we have

$$\|\text{diag}(\mathbf{g})\mathcal{H}(\mathbf{f})\text{diag}(\mathbf{h})\|_F \leq \|\mathbf{g}\|\|\mathbf{f}\|\|\mathbf{h}\|,$$

and then

$$\begin{aligned}
\tilde{\mathcal{L}}(\mathbf{g}^0, \mathbf{f}^0) &= \mathcal{L}(\mathbf{g}^0, \mathbf{f}^0) = \|\text{diag}(g^0)\mathcal{H}(\mathbf{f}^0)\text{diag}(\bar{\mathbf{g}}^0) - \text{diag}(g)\mathcal{H}(f)\text{diag}(\bar{g}) + R^y - \hat{R}^y\|_F \\
&\leq \|\mathbf{g}^0\|^2\|\mathbf{f}^0\| + \|g\|^2\|f\| + \|R^y - \hat{R}^y\|_F \leq 3\hat{n}_0 + \|R^y - \hat{R}^y\|_F.
\end{aligned} \tag{45}$$

Our gradient descent algorithm guarantees $\tilde{\mathcal{L}}(\mathbf{g}^k, \mathbf{f}^k) \leq \tilde{\mathcal{L}}(\mathbf{g}^0, \mathbf{f}^0)$, $k = 1, 2, \dots$ (see (46)). We will prove $(\mathbf{g}^k, \mathbf{f}^k) \in \mathcal{N}_{\hat{n}_0}$ by contradiction. Assume that $(\mathbf{g}^k, \mathbf{f}^k) \notin \mathcal{N}_{\hat{n}_0}$ for some k . Then

$$\tilde{\mathcal{L}}(\mathbf{g}^k, \mathbf{f}^k) \geq \rho \left[\mathcal{G}_0 \left(\frac{\|\mathbf{f}^k\|^2}{2\hat{n}_0} \right) + \mathcal{G}_0 \left(\frac{\|\mathbf{g}^k\|^2}{\sqrt{2\hat{n}_0}} \right) \right] > \rho\mathcal{G}_0(\sqrt{2}) = \rho(\sqrt{2} - 1)^2.$$

By taking $\rho \geq \frac{3\hat{n}_0 + \|R^y - \hat{R}^y\|_F}{(\sqrt{2} - 1)^2}$, we would have $\tilde{\mathcal{L}}(\mathbf{g}^k, \mathbf{f}^k) > 3\hat{n}_0 + \|R^y - \hat{R}^y\|_F$ which contradicts (45). We conclude that $(\mathbf{g}^k, \mathbf{f}^k) \in \mathcal{N}_{\hat{n}_0}$ at every iteration k .

Part 2: Let $\mathbf{z} = (\mathbf{g}, \mathbf{f})$ and $\Delta\mathbf{z} = (\Delta\mathbf{g}, \Delta\mathbf{f})$. Notice that $\tilde{\mathcal{L}}$ is continuously differentiable and real-valued. Suppose $\mathbf{z}, \mathbf{z} + \Delta\mathbf{z} \in \mathcal{N}_{\hat{n}_0}$. Then $\mathbf{z} + t\Delta\mathbf{z} \in \mathcal{N}_{\hat{n}_0}$ due to convexity of $\mathcal{N}_{\hat{n}_0}$.

It follows from Lemma 6.1 in [16] that, if $h(t) := \tilde{\mathcal{L}}(\mathbf{z} + t\Delta\mathbf{z})$, then

$$\frac{dh(t)}{dt} = (\Delta\mathbf{z})^T \frac{\partial \tilde{\mathcal{L}}}{\partial \mathbf{z}}(\mathbf{z} + t\Delta\mathbf{z}) + (\Delta\bar{\mathbf{z}})^T \frac{\partial \tilde{\mathcal{L}}}{\partial \bar{\mathbf{z}}}(\mathbf{z} + t\Delta\mathbf{z}) = 2\text{Re} \left((\Delta\mathbf{z})^T \overline{\nabla_{\mathbf{z}} \tilde{\mathcal{L}}(\mathbf{z} + t\Delta\mathbf{z})} \right).$$

By Fundamental Theorem of Calculus, we have

$$\begin{aligned} \tilde{\mathcal{L}}(\mathbf{z} + \Delta\mathbf{z}) - \tilde{\mathcal{L}}(\mathbf{z}) &= \int_0^1 \frac{dh(t)}{dt} dt = 2 \int_0^1 \text{Re} \left((\Delta\mathbf{z})^T \overline{\nabla_{\mathbf{z}} \tilde{\mathcal{L}}(\mathbf{z} + t\Delta\mathbf{z})} \right) dt \\ &\leq 2\text{Re} \left((\Delta\mathbf{z})^T \overline{\nabla_{\mathbf{z}} \tilde{\mathcal{L}}(\mathbf{z})} \right) + 2\|\Delta\mathbf{z}\| \int_0^1 \|\nabla_{\mathbf{z}} \tilde{\mathcal{L}}(\mathbf{z} + t\Delta\mathbf{z}) - \nabla_{\mathbf{z}} \tilde{\mathcal{L}}(\mathbf{z})\| dt \\ &\leq 2\text{Re} \left((\Delta\mathbf{z})^T \overline{\nabla_{\mathbf{z}} \tilde{\mathcal{L}}(\mathbf{z})} \right) + C_{\text{Lip}} \|\Delta\mathbf{z}\|^2. \end{aligned}$$

At the k th iteration, we let $\mathbf{z} = (\mathbf{g}^k, \mathbf{f}^k)$, and $\Delta\mathbf{z} = -\eta^k \nabla_{\mathbf{z}} \tilde{\mathcal{L}}(\mathbf{g}^k, \mathbf{f}^k)$, and then

$$\tilde{\mathcal{L}}(\mathbf{g}^{k+1}, \mathbf{f}^{k+1}) \leq \tilde{\mathcal{L}}(\mathbf{g}^k, \mathbf{f}^k) - (2 - C_{\text{Lip}}\eta^k)\eta^k \|\nabla_{\mathbf{z}} \tilde{\mathcal{L}}(\mathbf{g}^k, \mathbf{f}^k)\|^2. \quad (46)$$

As long as $\|\nabla_{\mathbf{z}} \tilde{\mathcal{L}}(\mathbf{g}^k, \mathbf{f}^k)\| > 0$ and $\eta^k < 2/C_{\text{Lip}}$, we have

$$\tilde{\mathcal{L}}(\mathbf{g}^{k+1}, \mathbf{f}^{k+1}) < \tilde{\mathcal{L}}(\mathbf{g}^k, \mathbf{f}^k),$$

which implies $\|\nabla_{\mathbf{z}} \tilde{\mathcal{L}}(\mathbf{g}^k, \mathbf{f}^k)\| \rightarrow 0$ as $k \rightarrow \infty$.

□

References

- [1] A. Ahmed, B. Recht and Justin Romberg, “Blind deconvolution using convex programming,” *IEEE Transactions on Information Theory* **60(3)**, pp.1711-1732, 2014.
- [2] T. Bendory and Y. C. Eldar, “non-convex phase retrieval from STFT measurements,” arXiv preprint arXiv:1607.08218, 2016.
- [3] E. J. Candès and C. Fernandez-Granda, “Towards a mathematical theory of super-resolution,” *Communications on Pure and Applied Mathematics* **67(6)**, pp.906-956, 2014.
- [4] E. J. Candès, X. Li and M. Soltanolkotabi, “Phase retrieval via Wirtinger flow: Theory and algorithms,” *IEEE Transactions on Information Theory* **61(4)**, pp.1985-2007, 2015.
- [5] Y. Chi, “Guaranteed blind sparse spikes deconvolution via lifting and convex optimization,” *IEEE Journal of Selected Topics in Signal Processing* **10(4)**, pp.782-794, 2016.
- [6] Y. Chi, L. L. Scharf, A. Pezeshki and A. R. Calderbank, “Sensitivity to basis mismatch in compressed sensing,” *IEEE Transactions on Signal Processing* **59(5)**, pp.2182-2195, 2010.
- [7] A. J. Den Dekker and A. Van den Bos, “Resolution: a survey,” *Journal of Optical Society of America A* **14(3)**, pp.547-557, 1997.
- [8] M. Duarte and R. G. Baraniuk, “Spectral compressive sensing,” *Applied and Computational Harmonic Analysis* **35(1)**, pp.111-129, 2013.

- [9] Y. C. Eldar, *Sampling Theory: Beyond Bandlimited Systems*, Cambridge University Press, 2015.
- [10] A. Fannjiang and W. Liao, “Coherence pattern-guided compressive sensing with unresolved grids”, *SIAM Journal on Imaging Sciences* **5(1)**, pp.179-202, 2012.
- [11] B. Friedlander and A. J. Weiss, “Eigenstructure methods for direction finding with sensor gain and phase uncertainties,” *Circuits, Systems, and Signal Processing* **9(3)**, pp.271-300, 1990.
- [12] R. J. LeVeque, *Finite difference methods for ordinary and partial differential equations: steady-state and time-dependent problems*, Society for Industrial and Applied Mathematics, 2007.
- [13] Y. Li and M. H. Er, “Theoretical analyses of gain and phase error calibration with optimal implementation for linear equispaced array,” *IEEE Transactions on Signal Processing* **54(2)**, pp.712-723, 2006.
- [14] Y. Li, K. Lee and Y. Bresler, “Optimal Sample Complexity for Blind Gain and Phase Calibration,” *Proceeding of 12th international conference on Sampling Theory and Applications*, 2017, to appear.
- [15] W. Liao and A. Fannjiang, “MUSIC for single-snapshot spectral estimation: Stability and super-resolution,” *Applied and Computational Harmonic Analysis* **40(1)**, pp.33-67, 2016.
- [16] X. Li, S. Ling, T. Strohmer and K. Wei, “Rapid, robust, and reliable blind deconvolution via non-convex optimization,” arXiv:1606.04933, 2016.
- [17] S. Ling and T. Strohmer, “Self-calibration and biconvex compressive sensing,” *Inverse Problems* **31(11)**, pp.115002, 2015.
- [18] J. Nocedal and S. Wright, *Numerical optimization*, Springer Science & Business Media, 2006.
- [19] A. Paulraj and Thomas Kailath, “Direction of arrival estimation by eigenstructure methods with unknown sensor gain and phase,” *IEEE International Conference on Acoustics, Speech, and Signal Processing (ICASSP)* Vol. 10. IEEE, 1985.
- [20] G. R. B. de Prony, “Essai Experimentale et Analytique”, *J. de L’Ecole Polytechnique* **2**, pp. 24-76, 1795.
- [21] R. Roy and T. Kailath, “ESPRIT-estimation of signal parameters via rotational invariance techniques,” *IEEE Transactions on acoustics, speech, and signal processing* **37(7)**, 984-995, 1989.
- [22] R. O. Schmidt, “A signal subspace approach to multiple emitter location and spectral estimation”, Ph.D. thesis, Stanford Univ., Stanford, CA, Nov. 1981.
- [23] R. O. Schmidt, “Multiple emitter location and signal parameter estimation”, *IEEE Transactions on Antennas and Propagation* **34(3)**, pp.276-280, 1986.
- [24] P. Stoica and R. L. Moses, *Introduction to spectral analysis*, Vol. 1. Upper Saddle River: Prentice hall, 1997.

- [25] J. Sun, Q. Qu and J. Wright, “A geometric analysis of phase retrieval,” *2016 IEEE International Symposium on Information Theory (ISIT)*, 2016.
- [26] J. Sun, Q. Qu and John Wright, “Complete dictionary recovery over the sphere I: Overview and the geometric picture,” *IEEE Transactions on Information Theory* **63(2)**, pp.853-884, 2017.
- [27] G. Tang, B. N. Bhaskar, P. Shah and B. Recht, “Compressed sensing off the grid,” *IEEE transactions on information theory* **59(11)**, pp.7465-7490, 2013.
- [28] J. A. Tropp, “An introduction to matrix concentration inequalities,” *Foundations and Trends in Machine Learning* **8.1-2**, pp.1-230, 2015.
- [29] G. Wang, G. B. Giannakis and Y. C. Eldar, “Solving systems of random quadratic equations via truncated amplitude flow,” arXiv preprint arXiv:1605.08285, 2016.
- [30] H. Weyl, “Das asymptotische Verteilungsgesetz der Eigenwerte linearer partieller Differentialgleichungen (mit einer Anwendung auf die Theorie der Hohlraumstrahlung),” *Mathematische Annalen* **71(4)**, pp.441-479, 1912.
- [31] M. P. Wylie, S. Roy and R. F. Schmitt, “Self-calibration of linear equi-spaced (LES) arrays,” *IEEE International Conference on Acoustics, Speech, and Signal Processing (ICASSP)* **1**, pp. 281-284, 1993.
- [32] M. P. Wylie, S. Roy, and H. Messer “Joint DOA Estimation and Phase Calibration of Linear Equispaced (LES) Arrays,” *IEEE Transactions on Signal Processing* **42(12)**, pp. 3449-3459, 1994.
- [33] Z. Tuo, Z. Wang and Han Liu, “A non-convex optimization framework for low rank matrix estimation,” *Advances in Neural Information Processing Systems*, 2015.